Title: Testosterone-Induced Metabolic Changes in Seminal Vesicle Epithelial cells Alter Plasma Components to Enhance Sperm Fertility

Authors: Takahiro Yamanaka[1], Zimo Xiao[1], Natsumi Tsujita[1], Mahmoud Awad[1,2], Takashi Umehara[1], Masayuki Shimada[1,3*]

Affiliations:

[1] Graduate School of Integrated Sciences for Life, Hiroshima University; Higashihiroshima, Hiroshima, Japan

[2] Department of Histology, Faculty of Veterinary Medicine, South Valley University; Qena, Egypt

[3] Graduate School of Innovation and Practice for Smart Society, Hiroshima University; Higashihiroshima, Hiroshima, Japan

*Corresponding author. Masayuki Shimada, Ph.D. E-mail: mashimad@hiroshima-u.ac.jp, Tel/Fax: (+81)-824-24-7899

One Sentence Summary: Testosterone induces ACLY expression in seminal vesicles, a key factor in forming seminal plasma to acquire *in vivo* fertilization ability of sperm.

Abstract:

Male factors account for almost half of the causes of infertility. In rodents and humans, most of the components of semen are supplied by the seminal vesicles, and they support male reproductive ability, but there are many unknown details. In this study, the metabolic changes in the seminal vesicle epithelial cells were focused on, and the mechanisms by which testosterone affects the seminal plasma composition were investigated. A factor that improves the linear motility of sperm was secreted from the seminal vesicles, which were synthesized in an androgen-dependent manner. Bioassays, gene expression, and flux analysis studies demonstrated that testosterone promotes glucose uptake in seminal vesicle epithelial cells via GLUT4, resulting in oleic acid synthesis. Oleic acid was shown to be taken up by sperm and to promote linear motility, thereby improving fertilization rates both *in vitro* and *in vivo*. ACLY was a critical factor in this metabolic change, which produces oleic acid and enhances their fertilization ability *in vivo*. In

conclusion, the critical role of testosterone-induced metabolic changes in the seminal vesicles is to ensure the synthesis of oleic acid, which is important for sperm fertilization *in vivo*. These findings provide new perspectives for the development of potential biomarkers of male fertility and advances in the treatment of male infertility.

Main Text:

INTRODUCTION

Infertility is defined by the World Health Organization (WHO) as the failure to conceive within 12 months despite contraceptive-free sexual intercourse. Its prevalence has increased over the decades and accounts for 17.5% of couples worldwide *(1)*. The male partner is thought to be solely or in combination responsible for 50% of infertility cases, and the male factor in the etiology of infertility is highly recognized. Male fertility depends largely on the quality of semen composed of sperm and seminal plasma and decreases with aging *(2–4)*.

Spermatogenesis occurs in the testes. While passing through the epididymis, sperm undergo a maturation process, but sperm do not fully acquire their fertilizing ability in the epididymis. *(5–7)*. Therefore, sperm collected from the epididymis cannot fertilize oocytes unless they acquire the ability to fertilize in *in vitro* and cannot maintain sustained liner motility required for migration from the uterus to the oviduct *(8, 9)*. Thus, when epididymal sperm are artificially inseminated to the cervix or uterus, fertilization rates are low *(10–12)*. However, when epididymal sperm are mixed with seminal plasma at the time of ejaculation or when sperm are exposed to seminal plasma *in vitro*, even for only a brief period, they acquire *in vivo* fertilization potential and are capable of passing through the female reproductive tract and fertilizing ovulated oocyte *in vivo* *(13)*. Thus, sperm formation occurs in the testis; they mature in the epididymis but only acquire the *in vivo* fertilization ability after exposure to seminal plasma.

Seminal plasma is mainly produced in the seminal vesicles (approximately 65-75%), with approximately 20-30% produced by the prostate, and small amounts secreted by the bulbourethral and urethral glands *(14)*. The mixing of seminal fluid with accessory reproductive gland fluid during ejaculation causes semen to clot and liquefy in humans and causes vaginal plug formation in rodents. Vaginal plugs not only inhibit continuous mating but also play a role in maintaining sperm in the uterus and ensuring male fertility *(13)*. TGFβ, a component of seminal plasma, increases antigen-specific Treg cells in the uterus of mice and humans, which induces immune tolerance, resulting in pregnancy *(15, 16)*. Furthermore, SVS2, secreted from the seminal vesicle, is also known to be required for sperm to escape attack by the female immune system in the uterus *(17)*. In addition, seminal plasma contains various biochemical components that support sperm metabolism, including lipids and organic acids. Differences in the relative size of the accessory

reproductive glands reflect differences in the seminal plasma composition. Accordingly, there are considerable differences in the properties of seminal plasma between animal species. Specifically, Rosecrans et al. *(18)* found significant differences in the levels of most biochemical components in seminal plasma compared to blood, with specific factors like fructose being rarely detected in blood but abundant in seminal plasma. Our previous studies *(19–21)* documented that seminal plasma also contains creatine and fatty acids taken up by sperm within minutes. These substances play crucial roles in regulating sperm metabolic pathways and enhancing sperm motility. These observations indicate that seminal plasma not only alters the female immune system to protect sperm but also directly influences sperm metabolic pathways, facilitating the transformation of sperm capable of *in vivo* fertilization.

Some specific factors that male accessory glands contribute to seminal plasma and impact male fertility have been elucidated. For example, surgical removal of seminal vesicles in male mice and rats was associated with infertility *(17, 22, 23)*. The observation that fructose *(24)* and citric acid *(25)* concentrations in seminal plasma of control mice and rats are higher than in castrated animals indicates that specific functions of the accessory glands might be affected by testicular-derived testosterone that is known to activate the intracellular androgen receptor (AR; NR3C4), required for gene regulation of transcription. AR-deficient mice have been found to be infertile *(26)*, and long-term administration of androgen receptor antagonists, like flutamide, abolished male fertility *(27, 28)*. AR-deficient mice and transcriptome analyses have identified specific targets of AR *(29, 30)*. In both mice and human, androgen levels decrease with aging, and their concentrations have been reported to cause a decrease in male fertility, especially ejaculated sperm motility. Therefore, the reduction of androgen concentrations may affect the metabolic mechanisms of the accessory reproductive glands and alter the composition of seminal plasma with aging. However, the metabolic mechanisms that impact sperm functions are governed by a complex of enzymatic reactions. Therefore, the intricate interplay between testosterone and seminal plasma synthesis in the accessory reproductive glands requires further investigation.

In this study, we first performed various bioassays to identify which accessory reproductive glands are essential for sperm fertility. Subsequently, comparative *in vivo* and *in vitro* analyses were performed using a hypoandrogenic model. In addition, biochemical and molecular techniques such as RNA-seq, flux analysis, mass spectrometry, and knockdown experiments were

96 employed. These analyses revealed that testosterone promotes the synthesis of oleic acid in
97 seminal vesicle epithelial cells and its secretion into seminal plasma, and the oleic acid ensures
98 the linear motility and fertilization ability of sperm.
99
100 **RESULTS**
101 **The effect of androgen-dependent changes in mouse seminal vesicle secretions on the**
102 **linear motility of sperm**
103 A direct comparison was conducted to clarify the effects of secretions from the prostate and
104 seminal vesicles on the motility parameters of epididymal sperm. Since it is difficult to collect the
105 ejaculated semen of mice, a pseudo-seminal plasma was prepared by preparing fluids from the
106 seminal vesicle secretion and homogenized prostate tissue (Fig.1A, Supplemental Fig.1A). When
107 seminal vesicle secretions were added to the HTF medium, the sperm motility, progressive motile,
108 the straight line velocity (VSL), and the percentage of linearity (LIN) values increased
109 significantly compared to when only prostate extract was used. However, the curvi-linear velocity
110 (VCL) did not change (Fig.1B-F). Meanwhile, the secretions from the prostate and seminal
111 vesicles did not affect the viscosity of the medium (Fig.1G). These results indicate that sperm
112 exposure to seminal plasma factors significantly improves sperm linear motility (high VSL and
113 LIN).
114 Androgens regulate the functions of seminal vesicles. Therefore, to elucidate whether the
115 seminal vesicle factors, which enhance sperm linear motility, are synthesized in an androgen-
116 dependent manner, bioassays were performed using seminal vesicle secretions collected from
117 control mice or mice treated daily for 7 consecutive days with flutamide, an androgen receptor
118 antagonist (Fig. 1H, Supplemental Fig.1B). The results showed that Motile, Progressive motile,
119 LIN, and VSL were significantly reduced in the sperm cultured in seminal vesicle secretions from
120 flutamide-treated (Flutamide) compared to the sperm cultured in seminal vesicle secretions from
121 controls (Ctrl) (Fig.1I-L). The reduction of VSL, Motile, and Progressive motile were also
122 significantly lower in the sperm treated with seminal vesicle secretions from over 12 months old
123 mice that showed low circular testosterone levels as compared with the sperm treated with seminal
124 vesicle secretions from young adult mice (3 months old mice) (Supplemental Fig.2A,B).
125 Furthermore, JC-1 staining to measure mitochondrial membrane potential, which is important for

126 sperm linear motility, showed a significantly lower percentage of high mitochondrial membrane
127 potential in sperm treated with the secretions of seminal vesicles from flutamide-treated mice and
128 over 12 months old mice (Fig.1M, Supplemental Fig.1C,D, Supplemental Fig.2C). Since
129 flutamide treatment and aging also affect spermatogenesis and sperm motility, it should be noted
130 that epididymal sperm donors differ from seminal vesicle donors (Fig. 1H). The baseline
131 information for the epididymal sperm used in the experiment showed that the sperm were normal
132 (Supplemental Fig.1A). These results indicated that androgen-dependent changes in seminal
133 vesicle functions alter the levels/activity of seminal vesicle secretion factors, which regulate
134 sperm linear motility. The changes in seminal vesicle functions were also induced by aging.
135

136 **Testosterone-androgen receptor activity suppresses the proliferation of seminal vesicle epithelial**
137 **cells**

138 To understand the difference between seminal vesicles that secrete factors for enhancing sperm
139 linear motility and those that are impaired in this function, we performed histological analysis of
140 seminal vesicles recovered from mice treated and non-treated with flutamide. In control mice, the
141 seminal vesicle epithelial cells were in a single layer, and androgen receptors were localized in the
142 nuclei of seminal vesicle epithelial cells (Fig.2A). However, in mice treated with continuous
143 administration of flutamide, seminal vesicle epithelial cells were multilayered, and the strong
144 accumulation of androgen receptors in nucleus was not observed (Fig.2A). To investigate the cause
145 of this multilayering of cells, we performed Ki67 staining, a marker of cell proliferation, and
146 apoptosis detection by TUNEL staining (Fig.2B). The results showed that the percentage of Ki67-
147 positive cells increased significantly after treatment with flutamide, but the percentage of TUNEL-
148 positive cells did not change, suggesting that the testosterone-androgen receptor pathway is
149 responsible for the inhibition of proliferation of seminal vesicle epithelial cells (Fig.2C). These
150 changes of abnormal morphology and high proliferation activity were also observed in seminal
151 vesicle of more than 12 months old mice that showed the low level of testosterone in serum
152 (Supplemental Figure 2D-F). Therefore, seminal vesicle epithelial cells were collected and cultured
153 in primary culture, as shown in Fig. 2D. The changes in cell number were counted, and the cell
154 cycle was analyzed by flow cytometry. When cultured without testosterone (c), the number of

155 seminal vesicle epithelial cells increased day-dependent manner. However, the addition of
156 testosterone significantly decreased the number of seminal vesicle epithelial cells during the 8-day
157 culture period in a concentration-dependent manner (Fig.2E). Flow cytometric analysis of the cell
158 cycle on day 7 showed that the G0/G1 phase was significantly increased. The G2/M1 phase was
159 significantly decreased by the addition of testosterone (Fig. 2F,G). These results indicate that the
160 testosterone-androgen receptor pathway inhibits seminal vesicle epithelial cells in cell division.

161

162 **Testosterone alters metabolic gene expression in seminal vesicle epithelial cells**

163 To better understand the roles of testosterone in suppressing the proliferation of seminal vesicle
164 epithelial cells, RNA sequencing was done using the epithelial cells cultured with or without
165 testosterone. DEG (Differential Expressed Genes) analysis revealed that a total of 23,459 genes
166 were identified, including 997 upregulated genes and 3463 downregulated genes in seminal
167 vesicle epithelial cells by testosterone relative to control (Fig.3A). Genes largely upregulated
168 by testosterone included those already reported in seminal vesicles *(17, 22, 31)*, such as the
169 Seminal Vesicle Secretion (*Svs*) family (*Svs1~6*), *Pate4*, *Spinkl*, *Ceacam10*, and *Sva* (Fig.3B,C).
170 Therefore, the primary culture of seminal vesicle epithelial cells used in this experiment was
171 considered to maintain the characteristics of seminal vesicle epithelial cells *in vivo*. Many genes
172 were downregulated by testosterone, and those with a high rate of variation included collagen
173 synthase and *Mmp2*, which are involved in extracellular matrix formation (Fig.3C). However,
174 KEGG analysis, rather than individual genes, was used to predict functions altered by
175 testosterone. It was found that the expression of genes involved in the metabolic pathway was
176 the most highly affected by testosterone (Fig.3D). Because there is a close relationship between
177 cell proliferation and metabolic activity and between metabolic substrates in seminal plasma and
178 sperm motility, we hypothesized that testosterone induced changes in seminal vesicle epithelial
179 cell metabolism alter the components of seminal plasma to mediate the enhancement of sperm
180 motility.

181

182 **Testosterone shifts the metabolic activity of seminal vesicle epithelial cells**

183 In the presence of testosterone, the addition of glucose significantly activated the extracellular

184 oxidation rate (ECAR) normalized by the total number of live cells compared to that in epithelial
185 cells cultured without testosterone (Fig.4A-C). However, there was no difference in the
186 Oligomycin-sensitive ECAR, indicating that testosterone may increase glucose metabolism but
187 does not enhance the expression of a group of enzymes involved in the glycolytic pathway. To
188 determine the metabolic fate of glycolytic end products, seminal vesicle epithelial cells were
189 cultured with and without testosterone. Subsequently, the concentrations of pyruvate and lactate
190 in the culture supernatant normalized by the total number of live cells were measured. The
191 addition of testosterone significantly decreased the pyruvate concentration; however, the lactate
192 concentration did not change significantly (Fig.4D,E). Therefore, we analyzed mitochondrial
193 metabolism using a flux analyzer, predicting that more glucose is metabolized, pyruvate is synthesized
194 in response to testosterone, and is further metabolized in the mitochondria. Unexpectedly, when
195 measuring mitochondrial respiratory metabolism normalized by the total number of live cells with
196 a Flux analyzer, the basal respiratory rate (the electron transport chain activity) was significantly
197 decreased by testosterone (Fig.4F-J). Oligomycin-sensitive respiration was also significantly
198 suppressed by exposure to testosterone. Furthermore, the FCCP uncoupled respiration and spare
199 respiration capacity were also significantly decreased in response to testosterone treatment. These
200 results suggest that testosterone does not reduce transient enzyme activity in mitochondria but
201 rather weakens the metabolic pathway of the mitochondrial TCA cycle and/or the electron
202 transport chain due to the changes in gene expression patterns in seminal vesicle epithelial cells.
203

204 **Testosterone causes changes in the expression of genes encoding enzymes involved in glucose**
205 **catabolism and anabolism**

206 The expression of genes involved in glucose catabolism and anabolism in the *in vitro* culture
207 system of seminal vesicle epithelial cells was analyzed by qPCR (Fig.5). The gene expression of
208 glucose transporter (*Glut*) and enzymes involved in the glycolytic pathway was not significantly
209 affected by testosterone, consistent with the results of metabolic flux analysis, which showed that
210 the glycolytic pathway was not enhanced despite the activation of the glycolysis. Furthermore,
211 testosterone did not significantly affect the expression of genes encoding enzymes involved in the
212 TCA cycle in mitochondria. However, the expression of enzymes involved in the electron
213 transport chain was significantly decreased. Interestingly, the expression of *Acly*, which encodes

214 an enzyme that reconverts citric acid formed in the TCA cycle to Acetyl CoA and induces
215 cholesterol and fatty acid synthesis, was significantly increased by testosterone. Although *Hmgcr*,
216 which encodes the rate-limiting enzyme involved in cholesterol synthesis, was unchanged, the
217 expression of *Acc*, which encodes the rate-limiting enzyme for fatty acid synthesis, was
218 significantly upregulated by testosterone. These characteristic testosterone-induced changes in
219 gene expression observed in cultured cells were also detected by ACLY immunostaining of *in*
220 *vivo* seminal vesicle samples (Supplemental Figure 3). Specifically, the expression of genes
221 encoding a group of enzymes of the electron transport chain was significantly upregulated by
222 continuous flutamide administration *in vivo*, whereas the gene expression of *Acly* and *Acc* was
223 significantly decreased by flutamide administration. Immunostaining results showed that ACLY
224 was detected specifically in seminal vesicle epithelial cells, and their staining appeared to be
225 reduced by flutamide treatment. The lower level of ACLY was also observed in seminal vesicle
226 epithelial cells of over 12 months old mice (Supplemental Figure 3B).
227
228 **Mechanism of testosterone-induced enhancement of glucose uptake and, thereby, fatty acid**
229 **synthesis**
230 Since it is known that testosterone regulates the intracellular localization of GLUT4, we
231 focused on the intracellular localization of GLUT4 and its glucose uptake capacity *(32, 33)*.
232 The effect of testosterone on glucose uptake in seminal vesicle epithelial cells was analyzed
233 using fluorescence-labeled glucose. As expected from the results of flux metabolic analyses,
234 testosterone treatment significantly increased glucose uptake (Fig.6A). Indinavir, a functional
235 inhibitor of GLUT4, significantly suppressed glucose uptake and significantly decreased fatty
236 acid synthesis (the amount of fatty acids accumulated in the cell), which was increased by
237 testosterone (Fig.6A,B).
238 Furthermore, immunostaining analysis of the localization of GLUT4 in seminal vesicles
239 revealed that GLUT4 was translocalized outside the nucleus of seminal vesicle epithelial cells
240 under the presence of testosterone (Fig.6C). These data suggest that GLUT4 was partially
241 localized at the plasma membrane and contributed to glucose uptake. In contrast, in seminal
242 vesicles from mice treated with flutamide continuously, no strong signal was detected at the
243 presumed location of GLUT4 near the plasma membrane of seminal vesicle epithelial cells, even

244 though the protein expression level was not affected (Fig.6C,D). The same characteristics were
245 observed in aged mice.
246 Qualitative and quantitative analysis of the fatty acids synthesis was performed by GC-MS.
247 In seminal vesicles, C16:0, C18:0, and C18:1 were detected, in which C18:1 was decreased to
248 an undetectable level in seminal vesicles of mice treated with the flutamide (Supplemental
249 Figure 4A). In the cultured seminal vesicle epithelial cells, C18:1, oleic acid, was significantly
250 increased by the addition of testosterone as observed in the seminal vesicle (Fig.6E). The
251 expression of *Elovl6* encoding ELOVL6, which desaturates C18:0 saturated fatty acids to C18:1,
252 was significantly up-regulated by testosterone (Fig.6F,G). The testosterone-induced change was
253 also detected in *in vivo* samples (seminal vesicle), where the expression of *Evovl6* was decreased
254 by the flutamide treatment (Supplemental Figure 4B).
255
256 **Oleic acid (18:1) is taken up by sperm and promotes their linear motility**
257 We observed that seminal vesicles secrete testosterone-dependent factors that induce sperm to
258 move linear and that seminal vesicle epithelial cells synthesize and secrete oleic acid in a
259 testosterone-dependent manner. In order to examine whether oleic acid is a factor that induces
260 sperm linear motility, we examined whether or not oleic acid is taken up by sperm and then
261 changes in sperm motility pattern. When epididymal sperm were incubated with fluorescently
262 labeled oleic acid, the fluorescent signal was selectively detected in the midpiece of the sperm
263 after quenching of extracellular fluorescence (Fig.7A). The fluorescence intensity of sperm
264 detected by flow cytometry significantly increased in a dose-dependent manner (Fig.7B, C).
265 Oleic acid did not affect sperm and progressive motile at any concentration compared to the
266 control (Fig.7D,E). In oleic acid-treated sperm, VSL was significantly increased in a dose-
267 dependent manner in the 0 to 50 nM (Fig.7F). LIN values were highest when 10 nM oleic acid
268 was added (Fig.7G). A flux analyzer was used to monitor real-time changes in mitochondrial β-
269 oxidation normalized by the number of sperm to quantify metabolic changes in mitochondrial
270 activity. The injection of 10 nM oleic acid induced a significant increase in OCR. Etomoxir, a β-
271 oxidation inhibitor, significantly decreased the OCR that was induced by oleic acid (Fig.7H,
272 Supplemental Figure 5A). In situ ATP detection by BioTracker ATP-Red revealed that the
273 percentage of sperm with high ATP production was significantly increased under the presence

274 of oleic acid (Fig.7I). To investigate the effect of oleic acid on the linear motility of sperm and
275 its effect on the fertilization ability of sperm, *in vitro* fertilization (IVF) was performed. When
276 the sperm number was sufficient, there was no change in the cleavage rate after *in vitro*
277 fertilization, but when the sperm count was reduced to less than one-tenth of the conventional
278 level, the cleavage rate increased compared to the control (Fig.7J,K). Due to the strong effect of
279 the decapacitation factor, we found that seminal vesicle fluid reduces the fertilization rate in IVF
280 (Supplemental Figure 5B). This results from inhibiting tyrosine phosphorylation of sperm and
281 acrosome reaction by seminal vesicle secretions. However, oleic acid did not have this inhibitory
282 effect (Supplemental Figure 5C-F).
283 To examine whether the addition of oleic acid to low quality seminal plasma (collected from
284 flutamide-treated mice) restores *in vivo* the fertilization potential of epididymal sperm, sperm
285 treated with seminal plasma collected from control or flutamide-treated mice was used for
286 artificial insemination. The *in vivo* fertilization rate was about 70% when sperm was treated with
287 the seminal vesicle secretions from control mice (SV); however, the fertilization rate was
288 significantly lower in the group that sperm was treated with the seminal vesicle secretions from
289 flutamide-treated mice (Flu) (SV: 73.1 ± 3.0%, Flu: 44.9 ± 4.5%). Although not significant,
290 adding oleic acid to the seminal secretions of flutamide-treated mice (Flu+OA) increased the
291 fertilization rate to 61.3 ± 3.9% (Fig.7L). These results indicated that the physiological role of
292 oleic acid is to increase the probability of fertilization by keeping the linear sperm motility. This
293 increases the likelihood of the sperm passing through the female reproductive tract and
294 environments that are unfavorable to sperm survival.
295
296 **ACLY expression is upregulated by testosterone and is essential for the metabolic shift of**
297 **seminal vesicle epithelial cells that mediates sperm linear motility**
298 ACLY is upregulated in seminal epithelial cells as a factor that enables the utilization of citric
299 acid from the TCA cycle for fatty acid synthesis outside the mitochondria. Therefore, we
300 performed siRNA knockdown experiments on ACLY to clarify the impact of ACLY on the
301 cellular metabolic shift. The addition of testosterone significantly increased the amount of ACLY
302 protein in seminal epithelial cells (Fig.8A,B). Viral infection with siRNAs encoding *Acly*-
303 targeted siRNAs markedly decreased the amount of ACLY (Fig.8C). When ACLY was knocked

304 down using shRNA, the proliferation arrest caused by testosterone was released, and the cells
305 began to proliferate again (Fig.8D). This knockdown of ACLY increased the oxygen
306 consumption of seminal epithelial cells in the control and testosterone-treated group (Fig.8E,F).
307 Thus, ACLY expression is associated with mitochondrial metabolic pathway activity in seminal
308 epithelial cells. Furthermore, the knockdown of ACLY also significantly suppressed
309 testosterone-induced fatty acid synthesis in seminal epithelial cells (Fig.8G). According to the
310 GC-MS quantification results, the amount of fatty acids secreted into the culture medium was
311 also reduced by ACLY knockdown. In particular, the enhancement of oleic acid secretion by
312 testosterone was inhibited by ACLY knockdown (Fig.8H-J). Supernatants from epithelial cells
313 of the testosterone-added group induced motility and linear motility (Highest VSL and LIN;
314 Fig.8K-N). However, the knockdown of ACLY significantly reduced the effects of the culture
315 supernatant on sperm motility and LIN (Fig.8K-N). These results found that cell proliferation
316 stops when a metabolic shift mediated by ACLY occurs, and glucose is reallocated to fatty acid
317 synthesis. Fatty acid synthesis is an important function of the seminal vesicles, and it was found
318 that when testosterone is present, fatty acid synthesis enhancement and cell proliferation stop
319 simultaneously. However, it is not known what effects occur when cell proliferation stops.
320

321 **This characteristic metabolic mechanism induced by testosterone is also observed in**
322 **human seminal epithelial cells**

323 To determine whether these findings in mice could be applied to humans, the commercially
324 available human seminal vesicle epithelial cells were used for following studies (Fig.9A). The
325 growth curves showed that cell proliferation was inhibited by 100 ng/mL of testosterone
326 compared to the control; a pattern similar to that observed in murine seminal vesicle epithelial
327 cells (Fig.9B). The characteristics of metabolic activity of human seminal epithelial cells were
328 also similar to those of mice, with testosterone significantly enhancing the ECAR response
329 (Fig.9C-E), but significantly reducing the capacity for oxygen consumption in mitochondria
330 (Fig.9F-H). Moreover, fluorescent-glucose uptake was increased by testosterone and decreased
331 by the inhibitor of GLUT4 function (Fig.9I). Additionally, while testosterone also significantly
332 increased fatty acid synthesis, this increase was completely abolished by the GLUT4 inhibitor
333 (Fig.9J). According to the quantitative results obtained using GC-MS, the amount of fatty acids

334 secreted into the culture medium also decreased due to the inhibition of GLUT4 by indinavir. In
335 particular, it was shown that oleic acid secretion is completely dependent on glucose via GLUT4
336 (Fig.9K-M).
337
338
339 **DISCUSSION**
340 Seminal plasma has a variety of functions, including sperm transport, nutritional support,
341 interactions with the female reproductive tract, and especially the regulation of its relationship
342 with the female immune system. Mammalian seminal plasma is secreted mainly from the
343 seminal vesicle and is rich in cytokines, prostaglandins, and SVS family members *(34)*. For this
344 reason, recent studies have focused on the immunomodulatory function of seminal plasma in the
345 female reproductive tract. On the other hand, fructose and lipids in seminal plasma are the major
346 energy sources for sperm *(35)*. However, although metabolomic analyses of seminal plasma
347 have shown that metabolic substrates are present at higher concentrations in seminal plasma than
348 in blood *(18, 24, 25)*, how these substrates are synthesized and specifically how they alter sperm
349 motility has not been determined. Moreover, though the motility of ejaculated spermatozoa is
350 known to decrease with aging, few reports have revealed age-related changes in the seminal
351 vesicles, which are responsible for seminal plasma synthesis.
352 In this study, we focused on the reproductive organs that synthesize seminal vesicle secretion
353 as target organs for testosterone and found that factors formed by testosterone-dependent
354 metabolic changes in seminal vesicles activate sperm mitochondria and enhance their linear
355 motility. Testosterone is known to activate intracellular ARs and alter intracellular metabolic
356 pathways in skeletal muscle *(36)*, prostate cells *(37)* and cardiomyocytes *(33)*. ARs are known
357 to directly regulate the expression of glycolytic and lipid metabolic genes *(33, 38, 39)*. In the
358 present study, the nuclear localization of AR in seminal vesicle epithelial cells (i.e., functioning
359 as a transcription factor) and the activation of the glycolytic system by testosterone were similar
360 to those in the above cell types. In seminal vesicle epithelial cells, an increased trend in the
361 expression of *Glut3* and an enhancement of GLUT4 function were observed in a testosterone-
362 dependent manner. Such effects of testosterone on glucose metabolism have also been reported
363 in skeletal muscle, liver, and adipose tissue, where testosterone leads to the phosphorylation of

364 GLUT4 and enhances its translocation to the plasma membrane *(40, 41)*. This is consistent with
365 the results of our metabolic flux analyses, which show that testosterone increases the rate of
366 glycolysis in seminal vesicle epithelial cells by increasing glucose uptake. We further confirmed
367 that GLUT4 is the transporter that mediates this glucose uptake using indinavir, a GLUT4-
368 specific inhibitor.

369 This study suggests that fatty acid synthesis is an important function of the seminal vesicles,
370 which provide an environment where the ejaculated sperm can carry out active metabolism. The
371 shift to fatty acid synthesis was consistent with the cessation of cell proliferation in the presence
372 of testosterone. This mechanism could prevent the seminal vesicles from excessively consuming
373 the substrates necessary for sperm motility. Manipulation of ACLY expression in mouse
374 myoblasts and embryonic stem cells has been shown to alter the TCA cycle into a "non-normal
375 cycle" *(42)*. One advantage of the non-normal TCA cycle is its ability to retain carbon instead
376 of combusting it and to regenerate the cytosolic NAD+ needed to maintain glycolysis *(42, 43)*.
377 It suggests that ACLY, activated by testosterone, may suppress proliferation by skipping several
378 steps in the mitochondrial TCA cycle and minimizing ATP production associated with aerobic
379 respiration in seminal vesicle epithelial cells.

380 Testosterone has been reported to cause hypertrophy of cardiac myocytes *(44, 45)*. Cell
381 hypertrophy is partly due to the accumulation of fatty acids in the cytoplasm, which causes
382 significant damage to cellular functions *(46, 47)*. On the other hand, normal cell hypertrophy,
383 especially in myofibers, involves the activation of signaling molecules such as Myc, hypoxia-
384 inducible factor, and Pi3k-Akt-mTor, which regulate metabolic reprogramming in cancer by
385 increasing glucose uptake in the presence of oxygen *(48–50)*. In the present study, induction of
386 ACLY expression by testosterone not only decreased cycling in the TCA cycle, but also promoted
387 glucose assimilation, which played an important role in fatty acid synthesis. Thus, in tissues
388 where fatty acid synthesis is promoted, either β-oxidation-dependent ATP production in
389 mitochondria or the secretion of fatty acids occurs to maintain cellular function *(51–53)*,
390 providing evidence to explain why the presence of fatty acids in the cell has no adverse effect.
391 In accessory reproductive glands, such as the prostate and seminal vesicles, the glucose uptake
392 is activated in a testosterone dependent. However, mitochondrial respiration is not enhanced,
393 cell proliferation is not induced, and the metabolites are used as a substrate for sperm motility.

394 This may be because, in the prostate, pyruvate synthesized by the glycolytic system in response
395 to testosterone is converted to acetyl CoA, which is then converted to citric acid in the TCA
396 cycle, citric acid is released as the main component of seminal plasma *(37)*.

397 The testosterone-dependent growth of cancerous prostate epithelial cells may be due to genetic
398 mutations, such as elevated expression of the gene encoding aconitase, which converts citric acid
399 to isocitrate, which blocks the TCA cycle and inhibits citric acid secretion *(54)*. On the other
400 hand, in the analysis of seminal epithelial cells, testosterone treatment induced the expression of
401 *Acc*, which encodes the rate-limiting enzyme for fatty acid synthesis, and *Elovl6*, which
402 desaturates to oleic acid, significantly increasing total saturated fatty acid and oleic acid content.
403 Therefore, testosterone promotes glucose conversion into fatty acids, especially oleic acid, in
404 seminal epithelial cells. Although there is a commonality in the activation of the glycolytic
405 system testosterone target tissues, the different expression patterns of genes involved in
406 metabolism in mitochondria may exert their specific functions in each tissue. In addition to genes
407 involved in fatty acid synthesis such as *Fasn* and *Elovl6*, *Acly* is also encoded in a region in close
408 proximity to human chromosome 17 and mouse chromosome 11, suggesting that in seminal
409 vesicle epithelial cells, this region is targeted to promote gene expression. The co-regulation of
410 these genes in seminal vesicle epithelial cells leads to synthesizing oleic acid that ensures sperm
411 motility and function.

412 Decreased testosterone synthesis in the testes is a phenomenon observed with aging associated
413 with decreased spermatogenesis *(55)*. However, the probability of obtaining sperm without ICSI
414 or IVF is extremely low, despite the presence of sufficient numbers of sperm with normal-
415 morphology *(56–58)*. This indicates that testosterone plays a major role not only in
416 spermatogenesis but also in the functional maturation of sperm. In this study, metabolic
417 abnormalities induced by inhibition of androgen receptor function caused abnormal proliferation
418 of seminal vesicle epithelial cells in aged mice. In other words, the findings of the seminal vesicle
419 epithelial cell culture experiments and flutamide treatment may mimic the changes that occur
420 with aging. Oleic acid synthesis by testosterone-dependent metabolic pathways was regulated in
421 seminal vesicle epithelial cells and the oleic acid stimulated sperm motility and enhanced *in vivo*
422 fertilization success. It could be assumed that a decrease in testosterone levels causes
423 abnormalities in the components of human semen. Specifically, the results open the possibility

424 of translational studies to understand human male infertility, especially in cases of failure to
425 conceive by natural mating or artificial insemination.
426 Because seminal plasma contains components specific to certain male reproductive organs,
427 differences in protein composition may reflect pathological processes in these specific organs
428 (59). However, although proteomic and metabolomic analyses of seminal plasma have been
429 performed (31, 59), the functional changes in seminal plasma, especially the effects on *in vivo*
430 fertilization potential, are not fully understood. Differences in fatty acid concentrations,
431 including oleic acid, in seminal plasma may provide a predictive marker for the fertilization
432 potential of both human and domestic animal semen. Furthermore, the addition of oleic acid to
433 low-quality semen improved fertilization rates associated with artificial insemination, offering a
434 strategy for improving artificial insemination. In our previous study, the addition of fatty acids
435 to the thawing medium of frozen bull sperm improved linear motility and viability *(21)*. The
436 similarities between mouse and human seminal vesicle epithelial cells demonstrated in this study
437 have strong potential for the clinical application of these observations.
438 Overall, the results of the studies described herein strongly support the hypothesis that
439 testosterone-dependent glucose to oleic acid conversion processes are required for normal
440 seminal plasma functions in the seminal vesicle and normal reproductive performance in males
441 (Fig.10). This study advances our understanding of the role of testosterone in glucose
442 metabolism and fatty acid synthesis and lays the groundwork for future research and potential
443 therapeutic interventions in reproductive biology and fertility.
444
445 **MATERIALS AND METHODS**
446 **Study design**
447 The objective of this study was to elucidate the mechanisms of sperm plasma synthesis that
448 enhance sperm fertility. Testosterone-dependent changes in the seminal plasma function were
449 examined by comparative analysis of adult mice and flutamide-treated mice. The bioassays of
450 extracts from male accessory glands by epididymal sperm motility analysis were used to examine
451 the seminal plasma components important for sperm fertilization. We also isolated the mouse
452 seminal vesicle epithelial cultured cells, and investigated the synthesis mechanism of the seminal

453 plasma components using RNA-seq, FluxAnalyzer, and shRNA knockdown. Finally, we
454 performed validation using the human epithelial cells.
455
456 **Chemicals and Animals**
457 Unless otherwise noted, chemicals used in this study were purchased from Sigma-Aldrich (St.
458 Louis, MO, USA) or Nacalai tesque (Osaka, Japan). Pregnant mare serum gonadotropin (PMSG)
459 and human chorionic gonadotropin (hCG) were purchased from Asuka Seiyaku (Tokyo, Japan).
460 All procedures during animal experiments were reviewed and approved by the Animal Care and
461 Use Committee of Hiroshima University (Hiroshima, Japan; C21-9-3) and conducted according
462 to regulations. Specific pathogen-free C57BL/6NCrl male mice or Crl: CD1 (ICR) female mice
463 were purchased from Jackson Laboratory Japan (Kanagawa, Japan) and housed in an
464 environmentally controlled room with a 12-hour light/dark cycle, a temperature of 23 ± 3°C, and
465 free access to laboratory food (MF; Oriental Yeast Co., Ltd., Tokyo, Japan) and tap water. 8- to
466 16-week-old male or female mice were used for the experiments. Flutamide-treated mice were
467 injected subcutaneously for 7 days with 50 μg/g (body weight) of flutamide dissolved in corn oil.
468 Vehicle-treated mice received 100 μL of corn oil subcutaneously for 7 days. The aged males were
469 12 to 16 months old.
470
471 **Bioassay using pseudo-seminal plasma and epididymal sperm**
472 Prostate (mixed anterior, dorsal, lateral, and ventral) and seminal vesicles were collected from
473 adult C57BL/6NCrl mice. Seminal vesicle secretions were obtained by pressing the seminal
474 vesicles immediately after euthanasia. Prostatic extracts were obtained by homogenizing the
475 prostate immediately after euthanasia. Seminal vesicle secretions and prostate extracts collected
476 from one male mouse were dissolved in 500 μL and 200 μL of mHTF medium without BSA *(60)*,
477 respectively, then centrifuged at 2000 × g for 5 min at room temperature, and the supernatant was
478 collected, and protein levels were determined. The seminal vesicle secretions from flutamide-
479 treated mice were also collected similarly.
480 Cauda epididymis sperm recovered from male mouse were dispersed in 500 μL of mHTF
481 without BSA drops and centrifuged at 300 × g, 3 min to wash out epididymis-derived factors. The
482 final protein concentration of prostate and seminal vesicle secretion was adjusted to 10 mg/mL.

483 An aliquot (2 mL) of the pooled prostate or seminal vesicle extracts was conducted the viscosity
484 measurement data using Tuning Fork Vibro Viscometers (SV-1A, A&D Company, Tokyo, Japan).
485 The epididymis sperm was mixed with seminal vesicle secretion and/or prostate extract as shown
486 in Fig.1 and Supplementary Figure 1. The samples were incubated at 37°C for 60 min in a
487 humidified atmosphere of 5% CO2 in air. Sperm motility patterns were then examined using
488 computer-assisted sperm analysis (CASA; HT CASA-Ceros II, Hamilton Thorne, Beverly, MA,
489 USA), with software version 1.11.9. The following sperm motility parameters were analyzed:
490 percentage of motile sperm (denoted by a path velocity >40 μm/s and a VSL >20%), percentage
491 of motile sperm with progressive motility (denoted by a path velocity >40 μm/s and a straightness
492 ratio >60%). Straight-Line Velocity; VSL: The distance between the first and last tracking points
493 of the sperm trajectory divided by the elapsed time. Curvi-Linear Velocity; VCL: The sum of the
494 distances between the centers of brightness in each frame divided by the elapsed time. Linearity;
495 LIN: Measures the straightness of the path. LIN is derived from the ratio of VSL/VCL multiplied
496 by 100.
497
498 **Serum testosterone levels**
499 The serum was separated from the clot by centrifugation at 1,500 × g for 15 min. Testosterone
500 levels in the serum samples were determined by a rodent testosterone ELISA test kit (ERKR7016,
501 Endocrine Technologies, Inc., Newark, CA, USA) according to the manufacturer's manual.
502
503 **Mitochondrial activity**
504 Mitochondrial activity of sperm was measured using a MitoPT® JC-1 Assay Kit (911, Immuno
505 Chemistry Technologies, LLC, Bloomington, MN, USA) according to our previous study *(20)*.
506 Briefly, sperm were incubated with 200 μL of working solution containing 5,5',6,6'-tetrachloro-
507 1,1',3,3'-tetraethylbenzimidazolyl carbocyanine iodide (JC-1) dye at 37 °C for 30 min in the dark.
508 Using 10 μM of antimycin control (A8674; Sigma) under the same incubation conditions, we
509 confirmed that the JC-1 reaction is sensitive to changes in membrane potential. The sperm
510 suspension was centrifuged and washed twice with the base medium. After washing, the sperm
511 pellet was resuspended in the base medium and analyzed with an Attune® NxT Acoustic Focusing
512 Cytometer (Thermo Fisher Scientific Inc., Waltham, MA, USA) using a 488 nm laser and a filter

513 with a bandwidth of 574/26 nm. The intensity of the average value was analyzed as the mean
514 fluorescence intensity (MFI) of JC-1 orange aggregates. A total of 100,000 sperm events were
515 analyzed. The sperm population is shown in Supplementary Figure 6.
516
517 ***In vitro* fertilization (IVF)**
518 3 weeks old CD1 female mice were injected intraperitoneally with 4IU eCG to stimulate
519 follicle development and 5 IU hCG at 48 hours later. COCs collected from the oviductal
520 ampulla 16 h after hCG injection were placed into 100 μL of human tubal fluid (HTF) medium.
521 Sperm were collected from the cauda epididymis of 15 weeks or older C57BL/6N male mice in
522 100 μL of HTF medium. After 60 min of incubation with or without treatments, the sperm were
523 added into HTF medium at a final concentration of 2×10^5 spermatozoa/mL for conventional
524 experiments or 1×10^4 10 nM OA treated sperm/mL, and coincubated with the COCs. After 6h
525 incubation, oocytes were washed three times thoroughly and cultured in 250 μL of KSOM
526 medium (MR 106-D; Sigma). The cleavage rate was determined on Day 1 (Day 0=day of IVF),
527 and the appearance of blastocysts was recorded on Day 5.
528
529 **Immunohistochemistry and immunofluorescence**
530 Seminal vesicles were fixed overnight in 4% (w/v) paraformaldehyde/PBS, dehydrated in 70%
531 (v/v) ethanol, and embedded in paraffin. Paraffin-embedded fixed sections (4 μm) were
532 deparaffinized and hydrated with xylene and ethanol, respectively. Some slides were stained with
533 hematoxylin and eosin (HE). For antigen retrieval, sections were placed in citrate buffer (pH 6.0),
534 microwaved until boiling and allowed to stand at the temperature of pre-boil (95°C) for 15
535 minutes. Sections were incubated with 3% (v/v) hydrogen peroxide in methanol to block
536 endogenous peroxidase and then incubated with Normal Goat Serum Blocking Solution for rabbit
537 antibody (S-1000, Vector Laboratories, Newark, CA, USA) to block nonspecific sites. The
538 sections were then incubated overnight with primary rabbit antibodies: anti-AR antibody (1:100;
539 ab133273; Abcam, Cambridge, UK), anti-Ki67 antibody (1:1000; ab15580; Abcam) or anti-
540 ACLY antibody (1:200; ab40793; Abcam). Positive signals were visualized by DAB (3,3′-
541 Diaminobenzidine, 040-27001, Fujifilm Wako, Osaka, Japan) using the VECTASTAINE
542 LifeABC kit (PK-6101, Vector Laboratories) according to the manufacturer's protocol. Apoptotic

543 cells (including fragmented DNA) were detected using the In Situ Cell Death Detection Kit POD
544 (11684817910, Roche Ltd., Basel, Switzerland). To avoid false-positive or false-negative results,
545 DNAse-treated sections were used as positive controls, and TdT-untreated sections were used as
546 negative controls for apoptosis.
547 Nuclei were visualized with hematoxylin (Sakura Finetek, Tokyo, Japan). Ki-67 and apoptotic
548 positive cells were quantified using ImageJ software (National Institutes of Health; Bethesda, MD,
549 USA), with software version 2.1.0/1.53u. Randomly selected sections were stained, and images
550 were obtained from randomly selected fields in each section. The positive percentage is defined
551 as the percentage of positively stained cells in the total number of epithelial cells evaluated. Only
552 positive staining was considered, regardless of staining intensity. For immunofluorescence, after
553 blocking nonspecific sites, the sections were incubated with a primary antibody: anti-GLUT4
554 antibody (1:200; ab33780; Abcam). After washing with 0.3% (v/v) Triton X-100 in PBS (-), Cy3-
555 labeled goat anti-rabbit IgG (1:200, C-2306, Sigma) and DAPI (VECTESHIELD Mounting
556 Medium with DAPI, H-1200, Vector Laboratories) were used to visualize the antigen and nuclei.
557 Digital images were taken using an APX100 Digital Imaging System and CellSens imaging
558 software (EVIDENT, Tokyo, Japan), with software version 4.1.1.
559
560 **Isolation and culture of seminal vesicle epithelial cells**
561 Seminal vesicles were removed from euthanized mice, cut open vertically to expose the seminal
562 vesicle cavity, and incubated with Hanks' balanced salt solution (HBSS; $CaCl_2 \cdot 2H_2O$ 0.185 g/L,
563 $MgSO_4$ 0.098 g/L, KCl 0.400 g/L, KH_2PO_4 0.060 g/L, NaHCO3 0.350 g/L, NaCl 8.000 g/L,
564 Na_2HPO_4 0.048 g/L, D-Glucose 1.0 g/L, dissolved in ultrapure water). Tissues were digested with
565 10 mL of HBSS containing 25 mg/mL pancreatin and 0.25% (v/v) trypsin EDTA for 1 hour at
566 4°C, 45 minutes at room temperature, and 15 minutes at 37°C, and epithelial cells were obtained.
567 These were passed through a 70 μm nylon filter (352350, Corning Inc., Corning, NY, USA) and
568 seeded into collagen-coated 12-well plates (4815-010, IWAKI, Shizuoka, Japan). Cells were
569 cultured in DMEM/F-12, 10% fetal bovine serum (FBS; 10438-018, Thermo Fisher Scientific
570 Inc.), 100 U/mL penicillin, 100 μg/mL streptomycin. The culture condition was 37°C, 5% CO_2,
571 95% air, and humidity.

572 Human seminal vesicle epithelial cells (4460, ScienCell Research Laboratories, Carlsbad, CA,
573 USA) were purchased, seeded in 2 μg/cm^2 poly-L-lysine-coated plates, and cultured in epithelial
574 cell medium (4101, ScienCell Research Laboratories). The cells were seeded at 10000 cells/cm^2
575 on collagen-coated plates the day before 100 ng/mL testosterone treatment. Testosterone was
576 dissolved in ethanol, and the final concentration of ethanol was adjusted to 0.1% (v/v) when used
577 for cultured cells. The culture medium was replaced every 48 hours.
578
579 **Cell proliferation curve**
580 The seminal vesicle epithelial cells were seeded at 10000 cells/cm^2 and then were cultured in
581 various concentrations of testosterone. The cells were washed with HBSS (without $CaCl_2$-
582 $2H_2O/MgSO_4$) at the time of cell counting and collected using 0.25% (v/v) trypsin. The recovered
583 cells were suspended in DMEM/F-12 medium, and cell numbers were determined using an
584 Automated Cell Counter TC20TM (BIO-RAD Laboratories, Hercules, CA, USA) to calculate the
585 number of cells contained per well (4 cm^2).
586
587 **Cell cycle analysis**
588 The recovered cells as described above were fixed in 2-5 ml of cold (4°C) 70% methanol for
589 at least 30 minutes on ice. After centrifugation at 500g for 5 minutes at 4°C to obtain pellets, the
590 cell pellet was suspended in 50 μM propidium iodide and 20 × diluted RNase (19101, QIAGEN
591 Inc., Venlo, Netherlands) and then were incubated at 37°C for 30 minutes. After twice washing
592 with 1 ml of PBS at 300 g for 3 min at 4°C, the cells were analyzed by flow cytometry. The cell
593 population is shown in Supplementary Figure 8. A total of 20,000 events were analyzed.
594
595 **RNA-sequencing**
596 Total RNA was extracted from cells using the RNeasy Mini Kit (74106, QIAGEN). Three
597 independent samples were assayed to evaluate the reproducibility of the experimental procedures.
598 The quality of total RNA (1 μg) submitted for sequencing was checked using a Bioanalyzer
599 (Agilent Technologies Inc., Santa Clara, CA, USA), and all RNA integrity numbers were >7.0.
600 The libraries for RNA sequencing were sequenced with 2 × 150-bp paired-end reads on a
601 NovaSeq6000 (Illumina Inc., San Diego, CA, USA). The obtained sequencing data were analyzed

602 using RaNA-seq *(61)*, an open bioinformatics tool for rapid RNA-seq data analysis. FASTQ files
603 were preprocessed in the pipeline using the Fastp tool, and expression was quantified using
604 Salmon. DEseq2 was used to identify differentially expressed genes (DEGs) with adjusted p-
605 values less than 0.05 between the testosterone-treated groups in transcripts per million (TPM)
606 between control and testosterone-treated cells. The pathways were identified from the KEGG
607 database on RaNA-seq.
608
609 **Extracellular flux analysis**
610 Oxygen consumption rate (OCR) and ECAR were measured using an extracellular flux
611 analyzer (XF HS Mini; Agilent Technologies). Eight-well plates for the XF HS Mini were coated
612 with fibronectin (5 μg/mL, F1141, Sigma-Aldrich) dissolved in phosphate-buffered saline (PBS),
613 incubated overnight, and then washed with Roswell Park Memorial Laboratory medium for XF
614 (Roswell Park Memorial Institute medium; RPMI, 103576-100, Agilent Technologies; containing
615 1% FBS) for XF before analysis. Mouse seminal vesicle epithelial cells or human seminal vesicle
616 epithelial cells treated with 100 ng/mL testosterone for 7 days were suspended in RPMI medium
617 at a concentration of 10,000 cells/180 μL, or mouse seminal vesicle epithelial cells infected with
618 shRNA were suspended at a concentration of 2000 cells/180 μL in each well. After centrifugation
619 at 300 × g for 3 minutes, the plates were placed in an incubator at 37°C and 100% air and used
620 for analysis within 1 hour.
621 For glucose metabolism assessment, cells were sequentially treated as indicated with D-
622 Glucose (10 mM; 103577-100, Agilent Technologies), Oligomycin (1 μM; O4876, Sigma-
623 Aldrich), and 2-Deoxy-Glucose (50 mM; D8375, Sigma-Aldrich).
624 For mitochondrial respiration measurement, cells were sequentially treated as indicated with
625 Oligomycin (1 μM), carbonyl cyanide 4-(trifluoromethoxy) phenylhydrazone (FCCP; 5 μM,
626 SML2959, Sigma-Aldrich), and Rotenone (1 μM; R8875, Sigma-Aldrich)/Antimycin A (1 μM;
627 A8674, Sigma-Aldrich). Cellular metabolism readouts, such as glycolysis, glycolytic reserve,
628 basal OCR, Maximum respiration, ATP Production, Spare respiratory capacity, were determined
629 using the Agilent Seahorse Wave software with software version 3.0.0.41. However, to avoid
630 many ambiguities and problems with interpretation, “glycolysis” is written as “Glucose-induced

631 ECAR", "glycolytic reserve" as "Oligomycin-sensitive ECAR", "maximum respiration" as
632 "FCCP uncoupled respiration", and "ATP production" as "Oligomycin-sensitive respiration".
633 For mouse sperm analysis, NaHCO3-free HTF medium was prepared according to Balbach et
634 al. *(62)*. Plates were coated with concanavalin A (0.5 mg/mL, Fujifilm Wako Chemicals)
635 overnight the day before assay. Each well was seeded with 180 μL of NaHCO3- Free HTF
636 medium containing 3,000,000 sperm cells. Sperm were injected with oleic acid (final
637 concentration: 10 nM) with or without etomoxir (final concentration: 40 nM, E1905, Sigma-
638 Aldrich).
639
640 **Measurement of pyruvate and lactic acid**
641 For measurements, mouse or human seminal vesicle epithelial cells were treated with 100
642 ng/ml testosterone for 6 days. The culture supernatant was collected after 24 hr of additional
643 culture. Pyruvate consumption was measured using the Pyruvate Assay kit (MET-5029, Cell
644 Biolabs, Inc., San Diego, CA, USA). The fluorescence intensity was measured using a microplate
645 reader (ex. 570 nm/em. 615 nm). Lactate released into the medium was measured using the
646 Lactate Assay kit (L256, DOJINDO LABOLATORIES Co., Ltd., Kumamoto, Japan). The
647 absorbance was measured using a microplate reader (wave length=450nm).
648
649 **qPCR**
650 The cDNA was synthesized from 40 ng of total RNA using oligo$(dT)_{15}$ primers (3805, Takara
651 Bio Inc., Shiga, Japan) and an Avian myeloblastosis virus (AMV) reverse transcriptase from
652 Promega (M5101, Madison, WI, USA). The cDNA and primers were added to Power SYBR
653 Green PCR Master Mix (4367659, Applied Biosystems, Foster City, CA, USA) in a total reaction
654 volume of 15 μl. Conditions were set to the following parameters: 10 min at 95°C, 15 sec at 95°C,
655 and 1 min at 60°C. Cycles were repeated 45 times. Specific primer pairs were selected and
656 analyzed, as shown in Table S1. Expression was first normalized to housekeeping gene *Rpl19*,
657 and fold change was calculated relative to the mean of the control samples.
658
659 **Glucose uptake test of seminal vesicle epithelial cells and lipid determination of culture**
660 **supernatants**

661 Mouse or human seminal vesicle epithelial cells treated with or without 100 ng/mL testosterone
662 for 6 days were used for this experiment. Cells were treated with or without the GLUT4 inhibitor
663 indinavir (100 nM) and 100 ng/mL testosterone for an additional 24 hours. Collected 15,000 cells
664 were subjected to Glucose Uptake Assay Kit-Green (UP02; DOJINDO), and fluorescence
665 intensity was measured using a microplate reader (ex. 485 nm/em. 535 nm).
666 Total lipid content in cultured medium was quantified using a lipid quantification kit (STA-617
667 Fluorometric, Cell Biolabs, Inc.) according to the manufacturer's protocol. The fluorescence
668 intensity was measured using a microplate reader (ex. 485 nm/em. 535 nm).
669
670 **Gas chromatography-mass spectrometry analysis**
671 Fatty acid measurements in culture supernatant and seminal vesicle secretions were done
672 according to our previous work *(21)*. Fatty acids in the samples were extracted and methylated
673 using a fatty acid methylation kit (06482-04, Nacalai Tesque) and then purified using a fatty acid
674 methyl ester purification kit (06483-94, Nacalai Tesque). The methylated sample (3.0 mL) was
675 dried and dissolved in 50 μL of elution solution. Samples were subjected to GC-MS.
676 Fatty acids were determined on an Agilent 7890A GC system coupled with a JMS-T 100 GCv
677 mass detector at the Natural Science Research Center, Hiroshima University (N-BARD). Sample
678 (1.0 μL aliquot) was injected to SP®-2560 capillary GC column (100 m × 0.25 mm i.d. × 0.2 μm
679 film thickness; 24056, Sigma-Aldrich). For measurements, helium was used as the carrier gas at
680 a constant flow rate of 2.0 mL/min. The GC oven temperature was gradually increased from
681 100°C to 300°C at a rate of 10°C/min and held at 300°C for 20 minutes. Ionization was performed
682 using electron ionization with an electron energy of 70 eV. Mass spectra were obtained in scan
683 mode (mass scan range 29-800 m/z). NIST MS Search v.2.0 was used to detect and identify of
684 fatty acids.
685
686 **Quantification of sperm oleic acid uptake by flow cytometry**
687 To detect the fluorescence intensity of each sperm sample using flow cytometry, sperm
688 collected from the epididymis were incubated with 1, 10 or 100 μM of fluorescently labeled oleic
689 acid (F-OA-01, NANOCS, New York, NY, USA). After washing, fluorescence were analyzed by
690 flow cytometry using a 530/30 nm bandwidth filter and measured as mean intensity. A total of

691 100,000 sperm events were analyzed. The localization of fluorescence in sperm was determined
692 using an APX100 Digital Imaging System.
693
694 **Evaluation of acrosome damage**
695 The acrosome status of sperm was assessed using 25 μg/mL fluorescein isothiocyanate-
696 conjugated peanut agglutinin (FITC-PNA; L7381, Sigma Aldrich, St. Louis, MO) and 2.4 nM
697 propidium iodide (PI; L 7011, Invitrogen) were used for evaluation. After incubation in the dark
698 at 37°C for 10 min. The fluorescence of FITC and PI were analyzed by flow cytometry using a
699 530/30 and 695/40 nm bandwidth filter, respectively. Damaged sperm were analyzed—FITC
700 fluorescence positive, but PI negative gate (Q4). A total of 100,000 sperm events were analyzed.
701 The sperm population is shown in Supplementary Figures 5 and 6.
702
703 **ACLY knock down experiment using shRNA**
704 The U6 shRNA lentiviral vector of the *Acly* gene (mAcly[shRNA#1]; a virus packaging service,
705 VectorBuilder, Chicago, IL, USA) was used for knockdown experiments. The ACLY sequence
706 targeted by the shRNA vector used in this study was 5′-GCAGCAAAGATGTTCAGTAAA-3′.
707 Lentivirally transduced cells were prepared according to manufacture protocol. Immediately after
708 isolation, the mouse seminal vesicle epithelial cells were cultured overnight in a medium
709 containing 5 μg/mL polybrene (VectorBuilder) and lentiviral particles expressing an shRNA
710 targeting ACLY or a scramble (Multiplicity of Infection of 10). After an additional overnight
711 incubation in a fresh culture medium, the cells were incubated for 5 days in a medium containing
712 1 μg/ml puromycin (19752-64, Nacalai tesque). 100 ng/mL of testosterone was added to all
713 procedures for the testosterone-treated group. Infection efficiency, calculated based on the
714 number of GFP-positive cells using an APX100 Digital Imaging System, ranged between 70%
715 and 90%.
716
717 **Western blot analysis**
718 Protein samples of mouse seminal vesicle epithelial cells, seminal vesicle tissue, and sperm
719 were prepared by homogenization in cell lysis buffer (04719964001, cOmplete™ Lysis-M
720 EDTA-free, Roche) and diluted with an equal volume of sample buffer solution containing 2-ME

721 (2 ×) for SDS-PAGE (30566-22, Nacalai tesque). The extracts (10 μg protein) were separated by
722 SDS-polyacrylamide gel (10%) electrophoresis and transferred to polyvinylidene fluoride
723 membranes (10600069, Cytiva, Tokyo, Japan). The membranes were then treated with Tris-
724 buffered saline and Tween 20 (TBST, 20 mM Tris, pH 7.5, 150 mM NaCl, 0.1% Tween 20)
725 containing 5% (w/v) Non-Fat Dry milk (MORINAGA MILK INDUSTRY Co., Ltd., Tokyo,
726 Japan) for the nonspecific reaction was blocked. When detecting phosphotyrosine, containing 5%
727 (w/v) bovine serum albumin was used as a blocking agent. The membranes were incubated
728 overnight at 4°C with primary antibodies: anti-phosphotyrosine antibody (1:10,000; 8959; Cell
729 Signaling), anti-GLUT4 antibody (1:100; ab33780; Abcam), anti-ACLY antibody (1:10,000;
730 ab40793; Abcam) or anti-α/β-Tubulin antibody (1:1,000; 2148S; Cell Signaling). The next day,
731 membranes were washed with TBST and incubated with HRP-labeled antibody specific for rabbit
732 IgG (1:4000; 7074S; Cell Signaling). The bands were visualized by using Enhanched
733 Chemiluminescence detection systems (RPN2232, Cytiva) and ChemiDoc^{TM} MP Imaging System
734 (BIO-RAD Laboratories). The bands were analyzed by using the software ImageJ. Densitometry
735 analysis was performed using the ImageJ Gel Analysis tool, and the background of the gel was
736 also removed individually for each band. The full-length blotting images are shown in
737 Supplementary Figure 7.
738
739 **ATP production in sperm**
740 After 1 hour of incubation in the presence or absence of oleic acid (10 nM), ATP in sperm was
741 visualized by BioTracker ATP-Red (SCT045, Sigma-Aldrich). The sperm were incubated with 10
742 nM of working solution containing BioTracker ATP-Red dye at 37 °C for 60 min in the dark.
743 After washing, the sperm pellet was resuspended in the base medium and analyzed with the flow
744 cytometry using a 488 nm laser and a filter with a bandwidth of 574/26 nm. A total of 100,000
745 sperm events were analyzed. The sperm population is shown in Supplementary Figure 6.
746
747 **Artificial insemination**
748 To examine the involvement of seminal vesicle secretions in fertilization, sperm from
749 C57BL/6N mice were injected directly into the uterine bodies of superovulated CD1 mice by
750 syringe, as previously described with minor modifications *(17, 22)*. CD1 female mice were

751 injected intraperitoneally with 8 IU eCG to stimulate follicle development and used as recipients
752 for artificial insemination 48 hours later. Artificial seminal fluid was prepared in HTF medium to
753 a final concentration of 10 mg/mL of collected control or frutamide-derived seminal vesicle
754 secretions. As rescue experiment, 10 nM of oleic acid was added to the frutamide-derived seminal
755 secretions. Cauda epididymis sperm was suspended with above artificial seminal fluid (1×10^6
756 sperm/mL), and a total of 40 μL (20 μL each per uterus) was injected through the cervix of the
757 female mice. After artificial insemination, 7.5 IU of hCG was injected to stimulate ovulation.
758 Subsequently, a mixture of vaseline and paraffin with a ratio of 10:1 was injected to form an
759 artificial plug around the cervix. After 36~48 hours of sperm injection, the putative eggs were
760 retrieved from the oviducts. The number of two-cell embryos and mature unfertilized eggs were
761 counted and used to estimate the fertilization success rate.
762
763 **Statistical analysis**
764 Quantitative data were presented as means ± SEM. The Bartlett's test was used to confirm
765 whether the variances were equal for each group in experiments consisting of three or more
766 groups. All statistical details of the experiments are given in the figure legends. R [(version
767 4.3.1 (2023-06-16)] was used for statistical analysis. Data were considered statistically
768 significant at $p < 0.05$.
769
770 **Data availability**
771 Nucleotide sequence data reported are available in the DDBJ Sequenced Read Archive under
772 the accession numbers DRA017090. Additional information needed to reanalyze the data
773 reported in this paper is available from the principal contact upon request.
774
775 **List of Supplementary Materials**
776 Supplemental Figures 1 to 8
777 Table S1
778 Supplementary Data
779
780 **Acknowledgments:**

The authors would like to thank JoAnne S. Richards for carefully proofreading the manuscript and useful comments.

Funding:

This work was supported in part by JSPS KAKENHI Grant Number 23H00361 to MS and 23K14069 to TU.

Author contributions:

Conceptualization: TY, TU, MS

Methodology: TY, ZX, NT, MA, TU

Investigation: TY, ZX, NT, MA, TU

Visualization: TY, MS

Funding acquisition: MS

Supervision: MS

Writing – original draft: TY

Writing – review & editing: TY, TU, MS

Competing interests:

MS holds stocks in and receives a salary from Hiroshima Cryopreservation Service Co. as a director. In addition, MS has received royalties and grants from Hiroshima Cryopreservation Service Co. M.S. has received consulting fees from Rohto Pharmaceutical Co., Ltd.. TU holds stocks in and receives a salary from Lullabio Inc. as a director and has received honoraria from Rohto Pharmaceutical Co., Ltd. The other authors declare they have no competing interests.

References

1. World Health Organization., Infertility prevalence estimates: 1990–2021. *Global report* , 1–98 (2023).

2. S. A. Kidd, B. Eskenazi, A. J. Wyrobek, Effects of male age on semen quality and fertility: a review of the literature. *Fertil Steril* **75**, 237–248 (2001).

3. A. Mumcu, A. Karaer, B. Dogan, G. Tuncay, Metabolomics analysis of seminal plasma

811 in patients with idiopathic Oligoasthenoteratozoospermia using high-resolution NMR
812 spectroscopy. *Andrology* **8**, 450–456 (2020).
813 4. Y. Xu, H. Lu, Y. Wang, Z. Zhang, Q. Wu, Comprehensive metabolic profiles of seminal
814 plasma with different forms of male infertility and their correlation with sperm parameters.
815 *J Pharm Biomed Anal* **177,** 112888 (2020).
816 5. S. Elbashir, Y. Magdi, A. Rashed, R. Henkel, A. Agarwal, Epididymal contribution to
817 male infertility: An overlooked problem. *Andrologia* **53**, e13721 (2021).
818 6. M. J. Cosentino, A. T. K. Cockett, Review Article: Structure and Function of the
819 Epididymis Transport of Spermatozoa. *Urol Res* **14**, 229–240 (1986).
820 7. B. Howarth, Fertilizing ability of cock spermatozoa from the testis epididymis and vas
821 deferens following intramagnal insemination. *Biol Reprod* **28**, 586–590 (1983).
822 8. S. Elbashir, Y. Magdi, A. Rashed, R. Henkel, A. Agarwal, Epididymal contribution to
823 male infertility: An overlooked problem. *Andrologia* **53**, e13721 (2021).
824 9. T. G. Cooper, Sperm maturation in the epididymis: A new look at an old problem. *Asian*
825 *J Androl* **9**, 533–539 (2007).
826 10. P. Gaddum-Rosse, Some observations on sperm transport through the uterotubal
827 junction of the rat. *Am J Anat* **160**, 333–341 (1981).
828 11. R. Shalgi, T. T. Smith, R. Yanagimachi2, A Quantitative Comparison of the Passage
829 of Capacitated and Uncapacitated Hamster Spermatozoa through the Uterotubal Junction.
830 *Biol Reprod* **46**, 419–424 (1992).
831 12. H. Li, P. Hung, S. S. Suarez, Ejaculated Mouse Sperm Enter Cumulus-Oocyte
832 Complexes More Efficiently In Vitro than Epididymal Sperm. *PLoS One* **21**, e0127753
833 (2015).
834 13. T. Noda, M. Ikawa, Physiological function of seminal vesicle secretions on male
835 fecundity. *Reprod Med Biol* **18**, 241–246 (2019).
836 14. P. Verze, T. Cai, S. Lorenzetti, The role of the prostate in male fertility, health and
837 disease. *Nat Rev Urol* **13**, 379–386 (2016).
838 15. E. Balandya, W. Wieland-Alter, K. Sanders, T. Lahey, Human Seminal Plasma Fosters
839 CD4+ Regulatory T-cell Phenotype and Transforming Growth Factor-β1 Expression.
840 *American Journal of Reproductive Immunology* **68**, 322–330 (2012).

841 16. T. Shima, K. Inada, A. Nakashima, A. Ushijima, M. Ito, O. Yoshino, S. Saito, Paternal
842 antigen-specific proliferating regulatory T cells are increased in uterine-draining lymph
843 nodes just before implantation and in pregnant uterus just after implantation by seminal
844 plasma-priming in allogeneic mouse pregnancy. *J Reprod Immunol* **108**, 72–82 (2015).
845 17. N. Kawano, N. Araki, K. Yoshida, T. Hibino, N. Ohnami, M. Makino, S. Kanai, H.
846 Hasuwa, M. Yoshida, K. Miyado, A. Umezawa, Seminal vesicle protein SVS2 is required
847 for sperm survival in the uterus. *Proc Natl Acad Sci U S A* **111**, 4145–4150 (2014).
848 18. R. R. ROSECRANS, R. S. JEYENDRAN, M. PEREZ-PELAEZ, W. P. KENNEDY,
849 Comparison of Biochemical Parameters of Human Blood Serum and Seminal Plasma.
850 *Andrologia* **19**, 625–628 (1987).
851 19. T. Umehara, T. Kawai, M. Goto, J. A. S. Richards, M. Shimada, Creatine enhances
852 the duration of sperm capacitation: a novel factor for improving in vitro fertilization with
853 small numbers of sperm. *Human Reproduction* **33**, 1117–1129 (2018).
854 20. Z. Zhu, T. Kawai, T. Umehara, S. A. M. Hoque, W. Zeng, M. Shimada, Negative
855 effects of ROS generated during linear sperm motility on gene expression and ATP
856 generation in boar sperm mitochondria. *Free Radic Biol Med* **141**, 159–171 (2019).
857 21. M. M. Islam, T. Umehara, N. Tsujita, M. Shimada, Saturated fatty acids accelerate
858 linear motility through mitochondrial ATP production in bull sperm. *Reprod Med Biol* **20**,
859 289–298 (2021).
860 22. T. Noda, Y. Fujihara, T. Matsumura, S. Oura, S. Kobayashi, M. Ikawa, Seminal vesicle
861 secretory protein 7, PATE4, is not required for sperm function but for copulatory plug
862 formation to ensure fecundity. *Biol Reprod* **100**, 1035–1045 (2019).
863 23. K. Queen, C. B. Dhabuwala, C. G. Pierrepoint, The effect of the removal of the
864 various accessory sex glands on the fertility of male rats. *J Reprod Fertil* **62**, 423–426
865 (1981).
866 24. Mann T, Studies on the metabolism of semen; fructose as a normal constituent of
867 seminal plasma; site of formation and function of fructose in semen. *Biochem J* **40**, 481–
868 491 (1946).
869 25. Humphrey GF, Mann T, Studies on the metabolism of semen; citric acid in semen.
870 *Biochem J* **44**, 97–105 (1949).

871 26. C. Chang, S. O. Lee, R. S. Wang, S. Yeh, T. M. Chang, Androgen receptor (AR)
872 physiological roles in male and female reproductive systems: lessons learned from AR-
873 knockout mice lacking AR in selective cells. *Biol Reprod* **89**, 1–16 (2013).
874 27. C. Fix, C. Jordan, P. Cano, W. H. Walker, Testosterone activates mitogen-activated
875 protein kinase and the cAMP response element binding protein transcription factor in
876 Sertoli cells. *Proc Natl Acad Sci U S A* **101**, 10919–10924 (2004).
877 28. K. Nagaosa, A. Kishimoto, R. Kizu, A. Nakagawa, A. Shiratsuchi, Y. Nakanishi,
878 Perturbation of spermatogenesis by androgen antagonists directly injected into
879 seminiferous tubules of live mice. *Reproduction* **133**, 21–27 (2007).
880 29. L. B. Smith, W. H. Walker, The regulation of spermatogenesis by androgens. *Semin*
881 *Cell Dev Biol* **30**, 2–13 (2014).
882 30. P. S. Cooke, W. H. Walker, Male fertility in mice requires classical and nonclassical
883 androgen signaling. *Cell Rep* **36**, 109557 (2021).
884 31. S. P. Smyth, B. Nixon, A. L. Anderson, H. C. Murray, J. H. Martin, L. A. MacDougall,
885 S. A. Robertson, D. A. Skerrett-Byrne, J. E. Schjenken, Elucidation of the protein
886 composition of mouse seminal vesicle fluid. *Proteomics* **22**, e2100227 (2022).
887 32. H. Murata, P. W. Hruz, M. Mueckler, Indinavir inhibits the glucose transporter isoform
888 Glut4 at physiologic concentrations. *AIDS* **16**, 859–863 (2002).
889 33. C. Wilson, A. Contreras-Ferrat, N. Venegas, C. Osorio-Fuentealba, M. Pávez, K.
890 Montoya, J. Durán, R. Maass, S. Lavandero, M. Estrada, Testosterone increases GLUT4-
891 dependent glucose uptake in cardiomyocytes. *J Cell Physiol* **228**, 2399–2407 (2013).
892 34. G. F. Gonzales, Function of seminal vesicles and their role on male fertility. *Asian J*
893 *Androl* **3**, 251–258 (2001).
894 35. A. Lenzi, M. Picardo, L. Gandini, F. Dondero, Lipids of the sperm plasma membrane:
895 from polyunsaturated fatty acids considered as markers of sperm function to possible
896 scavenger therapy. *Hum Reprod Update* **2**, 246–256 (1996).
897 36. M. T. Haren, A. M. Siddiqui, H. J. Armbrecht, R. T. Kevorkian, M. J. Kim, M. J. Haas,
898 A. Mazza, V. B. Kumar, M. Green, W. A. Banks, J. E. Morley, Testosterone modulates
899 gene expression pathways regulating nutrient accumulation, glucose metabolism and
900 protein turnover in mouse skeletal muscle. *Int J Androl* **34**, 55–68 (2011).

901 37. L. C. Costello, R. B. Franklin, Testosterone and prolactin regulation of metabolic
902 genes and citrate metabolism of prostate epithelial cells. *Horm Metab Res* **34**, 417–424
903 (2002).
904 38. K. Gonthier, R. T. K. Poluri, É. Audet-Walsh, Functional genomic studies reveal the
905 androgen receptor as a master regulator of cellular energy metabolism in prostate cancer.
906 *J Steroid Biochem Mol Biol* **191**, 105367 (2019).
907 39. M. F. Troncoso, M. Pavez, C. Wilson, D. Lagos, J. Duran, S. Ramos, G. Barrientos,
908 P. Silva, P. Llanos, C. Basualto-Alarcón, B. D. Westenbrink, S. Lavandero, M. Estrada,
909 Testosterone activates glucose metabolism through AMPK and androgen signaling in
910 cardiomyocyte hypertrophy. *Biol Res* **54**, 1–16 (2021).
911 40. Chen X, Li X, Huang HY, Li X, Lin JF, Effects of testosterone on insulin receptor
912 substrate-1 and glucose transporter 4 expression in cells sensitive to insulin. *Zhonghua Yi*
913 *Xue Za Zhi* **86**, 1474–1477 (2006).
914 41. K. Sato, M. Iemitsu, K. Aizawa, R. Ajisaka, Testosterone and DHEA activate the
915 glucose metabolism-related signaling pathway in skeletal muscle. *Am J Physiol*
916 *Endocrinol Metab* **294**, E961–E968 (2008).
917 42. P. K. Arnold, B. T. Jackson, K. I. Paras, J. S. Brunner, M. L. Hart, O. J. Newsom, S.
918 P. Alibeckoff, J. Endress, E. Drill, L. B. Sullivan, L. W. S. Finley, A non-canonical
919 tricarboxylic acid cycle underlies cellular identity. *Nature* **603**, 477–481 (2022).
920 43. A. Luengo, Z. Li, D. Y. Gui, L. B. Sullivan, M. Zagorulya, B. T. Do, R. Ferreira, A.
921 Naamati, A. Ali, C. A. Lewis, C. J. Thomas, S. Spranger, N. J. Matheson, M. G. Vander
922 Heiden, Increased demand for NAD+ relative to ATP drives aerobic glycolysis. *Mol Cell*
923 **81**, 691–707 (2021).
924 44. B. B. Yeap, Testosterone and cardiovascular disease risk. *Curr Opin Endocrinol*
925 *Diabetes Obes* **22**, 193–202 (2015).
926 45. J. D. Marsh, M. H. Lehmann, R. H. Ritchie, J. K. Gwathmey, G. E. Green, R. J.
927 Schiebinger, Androgen receptors mediate hypertrophy in cardiac myocytes. *Circulation*
928 **98**, 256–261 (1998).
929 46. G. F. Grabner, H. Xie, M. Schweiger, R. Zechner, Lipolysis: cellular mechanisms for
930 lipid mobilization from fat stores. *Nat Metab* **3**, 1445–1465 (2021).

931 47. B. Mittendorfer, Origins of metabolic complications in obesity: adipose tissue and
932 free fatty acid trafficking. *Curr Opin Clin Nutr Metab Care* **14**, 535–541 (2011).
933 48. H. Wackerhage, I. J. Vechetti, P. Baumert, S. Gehlert, L. Becker, R. T. Jaspers, M. H.
934 de Angelis, Does a Hypertrophying Muscle Fibre Reprogramme its Metabolism Similar
935 to a Cancer Cell? *Sports Med* **52**, 2569–2578 (2022).
936 49. R. J. De Berardinis, N. S. Chandel, Fundamentals of cancer metabolism. *Sci Adv* **2**,
937 e1600200 (2016).
938 50. G. L. Semenza, Hypoxia-inducible factors in physiology and medicine. *Cell* **148**,
939 399–408 (2012).
940 51. B. Morant-Ferrando, D. Jimenez-Blasco, P. Alonso-Batan, J. Agulla, R. Lapresa, D.
941 Garcia-Rodriguez, S. Yunta-Sanchez, I. Lopez-Fabuel, E. Fernandez, P. Carmeliet, A.
942 Almeida, M. Garcia-Macia, J. P. Bolaños, Fatty acid oxidation organizes mitochondrial
943 supercomplexes to sustain astrocytic ROS and cognition. *Nature Metabolism 2023 5:8* **5**,
944 1290–1302 (2023).
945 52. M. Duta-Mare, V. Sachdev, C. Leopold, D. Kolb, N. Vujic, M. Korbelius, D. C. Hofer,
946 W. Xia, K. Huber, M. Auer, B. Gottschalk, C. Magnes, W. F. Graier, A. Prokesch, B.
947 Radovic, J. G. Bogner-Strauss, D. Kratky, Lysosomal acid lipase regulates fatty acid
948 channeling in brown adipose tissue to maintain thermogenesis. *Biochim Biophys Acta*
949 *Mol Cell Biol Lipids* **1863**, 467–478 (2018).
950 53. S. C. C. Huang, B. Everts, Y. Ivanova, D. O'Sullivan, M. Nascimento, A. M. Smith,
951 W. Beatty, L. Love-Gregory, W. Y. Lam, C. M. O'Neill, C. Yan, H. Du, N. A. Abumrad,
952 J. F. Urban, M. N. Artyomov, E. L. Pearce, E. J. Pearce, Cell-intrinsic lysosomal lipolysis
953 is essential for alternative activation of macrophages. *Nat Immunol* **15**, 846–855 (2014).
954 54. K. H. Tsui, T. H. Feng, Y. F. Lin, P. L. Chang, H. H. Juang, p53 downregulates the
955 gene expression of mitochondrial aconitase in human prostate carcinoma cells. *Prostate*
956 **71**, 62–70 (2011).
957 55. S. Almeida, L. Rato, M. Sousa, M. G. Alves, P. F. Oliveira, Fertility and Sperm Quality
958 in the Aging Male. *Curr Pharm Des* **23**, 4429–4437 (2017).
959 56. T. Murata, Y. Ishitsuka, K. Karouji, H. Kaneda, H. Toki, Y. Nakai, S. Makino, R.
960 Fukumura, H. Kotaki, S. Wakana, T. Noda, Y. Gondo, β-cateninC429S mice exhibit

961 sterility consequent to spatiotemporally sustained Wnt signalling in the internal genitalia.
962 *Scientific Reports 2014 4:1* **4**, 1–7 (2014).
963 57. B. A. Stone, A. Alex, L. B. Werlin, R. P. Marrs, Age thresholds for changes in semen
964 parameters in men. *Fertil Steril* **100**, 952–958 (2013).
965 58. J. L. Frattarelli, K. A. Miller, B. T. Miller, K. Elkind-Hirsch, R. T. Scott, Male age
966 negatively impacts embryo development and reproductive outcome in donor oocyte
967 assisted reproductive technology cycles. *Fertil Steril* **90**, 97–103 (2008).
968 59. A. P. Drabovich, P. Saraon, K. Jarvi, E. P. Diamandis, Seminal plasma as a diagnostic
969 fluid for male reproductive system disorders. *Nat Rev Urol* **11**, 278–288 (2014).
970 60. T. Umehara, N. Tsujita, Z. Zhu, M. Ikedo, M. Shimada, A simple sperm-sexing
971 method that activates TLR7/8 on X sperm for the efficient production of sexed mouse or
972 cattle embryos. *Nat Protoc* **15**, 2645–2667 (2020).
973 61. C. Prieto, D. Barrios, RaNA-Seq: Interactive RNA-Seq analysis from FASTQ files to
974 functional analysis. *Bioinformatics* **36**, 1955–1956 (2019).
975 62. M. Balbach, J. Buck, L. R. Levin, Using an Extracellular Flux Analyzer to Measure
976 Changes in Glycolysis and Oxidative Phosphorylation during Mouse Sperm Capacitation.
977 *J Vis Exp* **2020**, e60815 (2020).
978
979
980
981

982 **Figures and Figure legends**

983 **Fig.1**

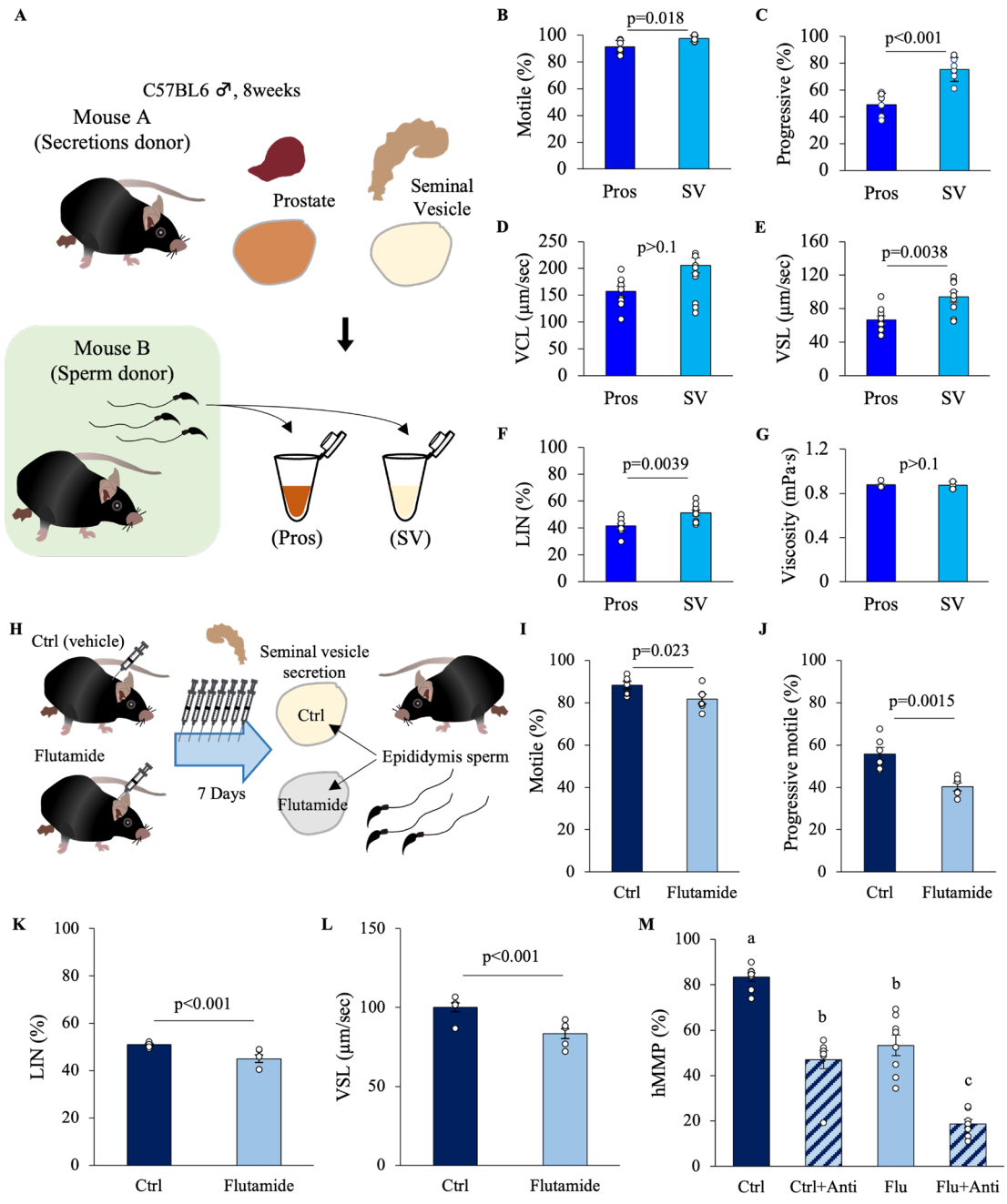

984

985

986

987

988

989

990 **Figure 1. Effects of seminal vesicle fluid and prostate fluids on sperm motility** (A) The effects
991 of secretions from the prostate and seminal vesicles on sperm motility were directly compared.
992 (B-F) The effects of secretions from the prostate (Pros) or seminal vesicles (SV) on the motility
993 parameters of epididymal sperm were tested: (B) Motile, (C) Progressive motile, (D) Curvi-
994 Linear Velocity; VCL, (E) Straight-Line Velocity; VSL and (F) Linearity; LIN is the ratio of VSL
995 to VCL of sperm that was incubated with the mixture of seminal vesicle secretions or prostate
996 extracts. (G) Viscosity of a solution containing prostate or seminal vesicle secretion with a protein
997 concentration of 10 mg/mL. (H) Experimental design to evaluate the effect of seminal vesicle
998 secretions collected from male mice treated with or without flutamide (50 mg/kg subcutaneously
999 every day for 7 days) on sperm. Note that the donor mice for sperm and seminal vesicle secretions
1000 were different. (I-L) Performed bioassay using seminal vesicle fluid after treatment with vehicle
1001 (Ctrl) or flutamide: (I) Motile, (J) Progressive motile, (K) LIN, (L) VSL. (M) The high
1002 mitochondrial membrane potential (hMMP) was checked by the JC-1 kit. Antimycin (Anti) was
1003 used as the negative control for hMMP. Data are mean ± SEM. n=3-9 independent replicates. The
1004 viscosity measurement data were from n=3 repeated experiments using pooled prostate or seminal
1005 vesicle extracts from at least 20 mice. Percentage data were subjected to arcsine transformation
1006 before statistical analysis. (B-G, I-L) Significance was tested in comparison using Student's t-test.
1007 (M) Since the results of the Bartlett test were significant, a two-way ANOVA using a generalized
1008 linear model was performed. Both the flutamide administration and antimycin addition were
1009 significant. The interaction was not significant. Games-Howell was performed as a post hoc test.
1010 Different letters represent significantly different groups.
1011
1012
1013

1014 **Fig.2**

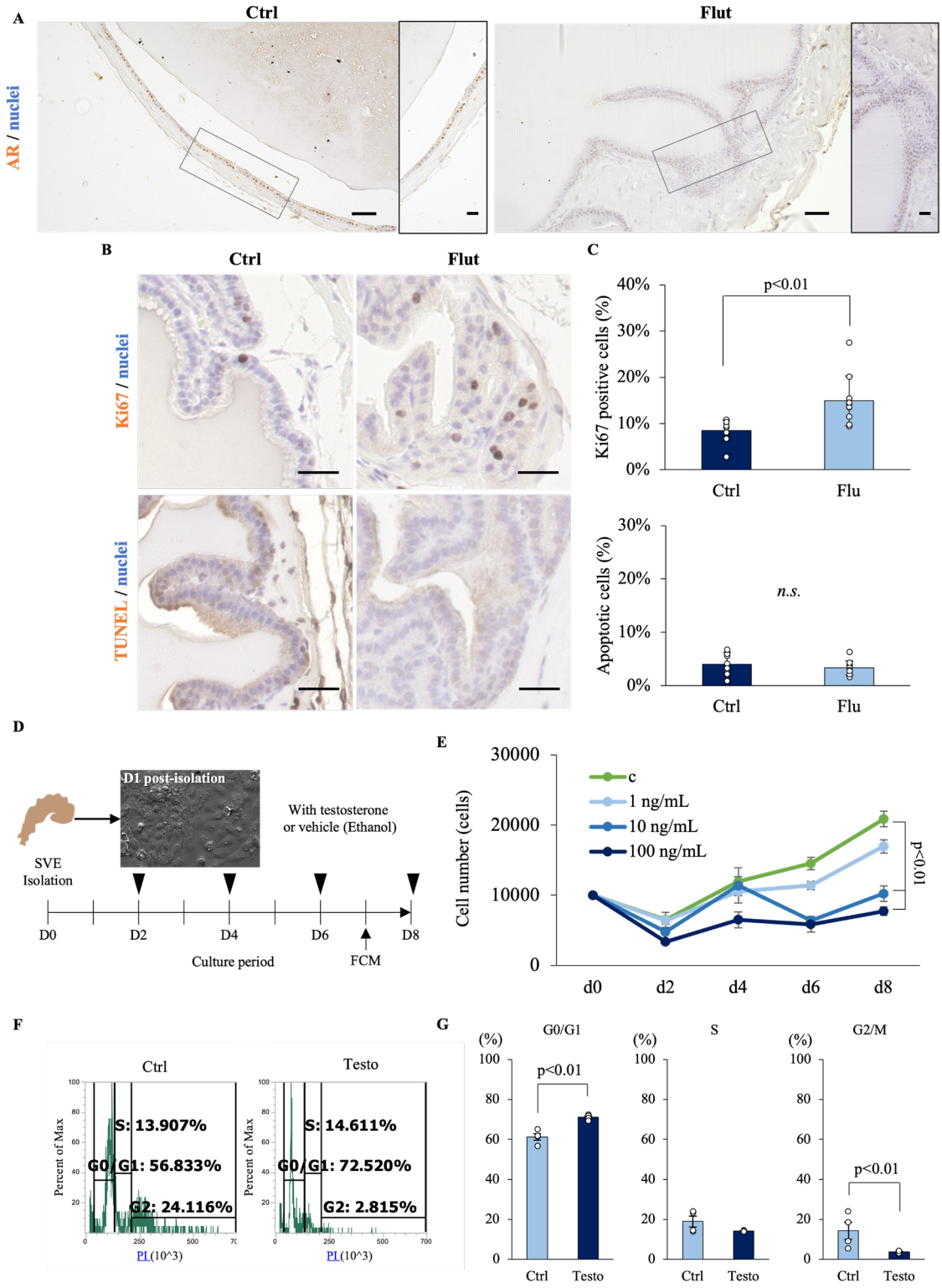

1015

1016

1017 **Figure 2. The testosterone-androgen receptor pathway inhibits the cell proliferation of**
1018 **seminal vesicle epithelial cells.** (A) The localization of the androgen receptor (AR; NR3C4) in
1019 seminal vesicle of control (Ctrl) mice and those treated with flutamide (Fult). Scale bar=50 μm
1020 from 10× magnification for left panel and 20 μm from 20× magnification for right panel in each
1021 group. (B,C) Cell proliferation and apoptosis in seminal vesicle of control (Ctrl) mice and those
1022 treated with flutamide (Fult): (B) Representative images of Ctrl and Flut staining for Ki67 (top)
1023 and TUNEL (bottom). Scale bar=20 μm. (C) Percentage of Ki67 positive cells (top) and TUNEL
1024 positive (bottom) in Ctrl and Flut-treated seminal vesicle sections. (D) Experimental design to
1025 evaluate the effects of testosterone on the proliferation of seminal vesicle epithelial cells *in vitro*.
1026 The epithelial cells were culutured with or without testosterone for 8 days. (E) Growth curves of
1027 seminal vesicle epithelial cells that cultured with 0 (c), 1, 10 and 100 ng/mL of testosterone. (F,G)
1028 Cell cycle status was determined by flow cytometry. Data are mean ± SEM. n=3-5 mice or
1029 independent replicates. Each replicate experiments with 3-6 wells containing pooled cells from
1030 3-5 mice. Percentage data were subjected to arcsine transformation before statistical analysis.
1031 Significance was tested in comparison to Ctrl using Student's t-test. The cell number data at d8
1032 was compared with the control using Dunnett's test.
1033
1034

1035 **Fig.3**

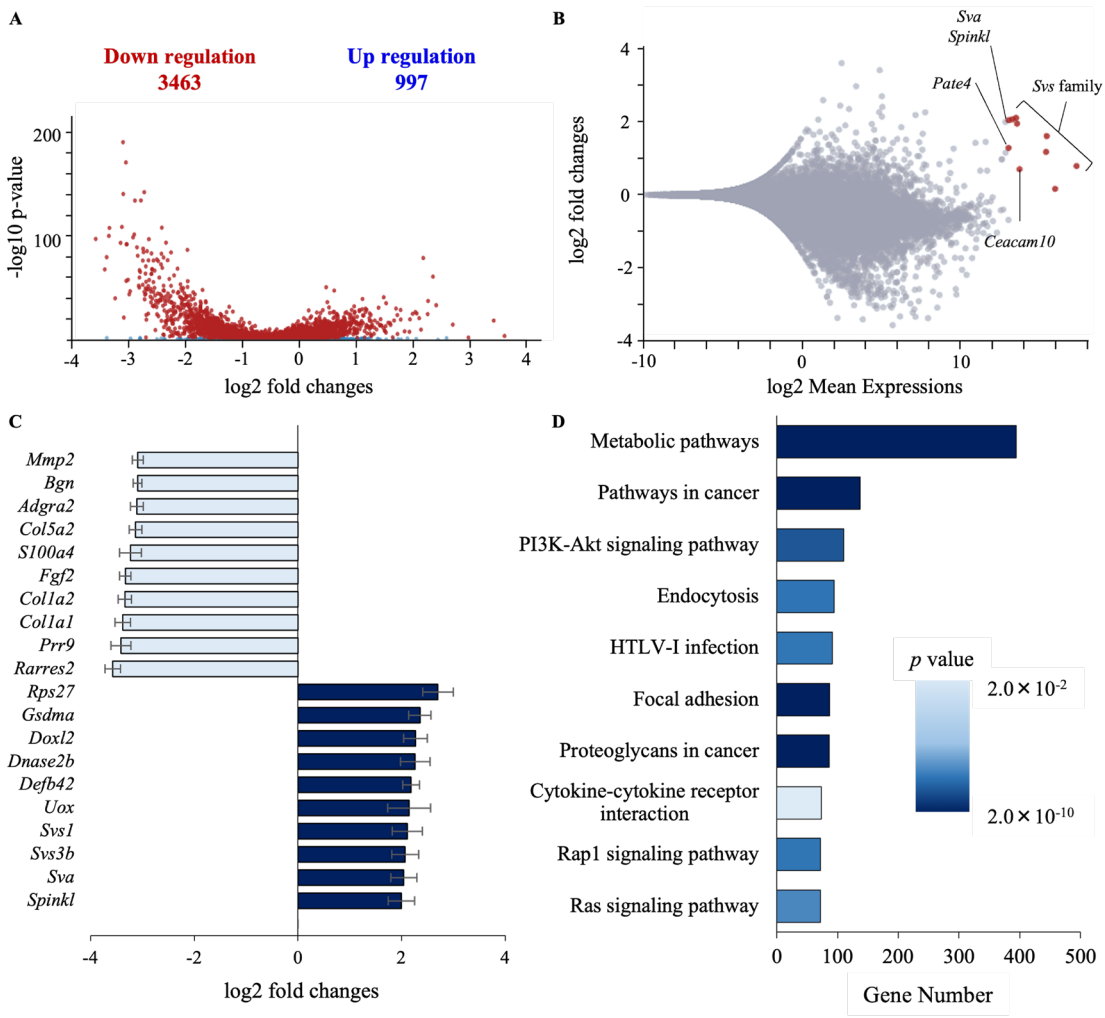

1036

1037 **Figure 3. Testosterone changes the expression of genes involved in metabolic pathway in**
1038 **seminal vesicle epithelial cells.** (A) Volcano plot of differentially expressed genes. RNA
1039 sequencing was performed using RNA extracted from the seminal vesicle epithelial cells cultured
1040 with or without 100 ng/mL testosterone. Genes with a significant expression change are
1041 highlighted as red dots. It found 4460 significant genes for a cutoff of P<0.05. (B) MA plot of
1042 differential expression results. The seminal vesicle specific genes are highlighted as red dots
1043 rather than significant genes. (C) Top 10 genes upregulated or downregulated by testosterone,
1044 respectively, for altered gene expression. (D) Conducted KEGG analysis to identify differences
1045 in pathway enrichment by testosterone, identifying the most variability in metabolic pathway
1046 genes. It shows the number of differential expressed genes annotated to Gene Ontology shows (x

1047 axis). p-value which measure the statistical significance of a possible functional enrichment for
1048 each term.
1049

1050 **Fig.4**

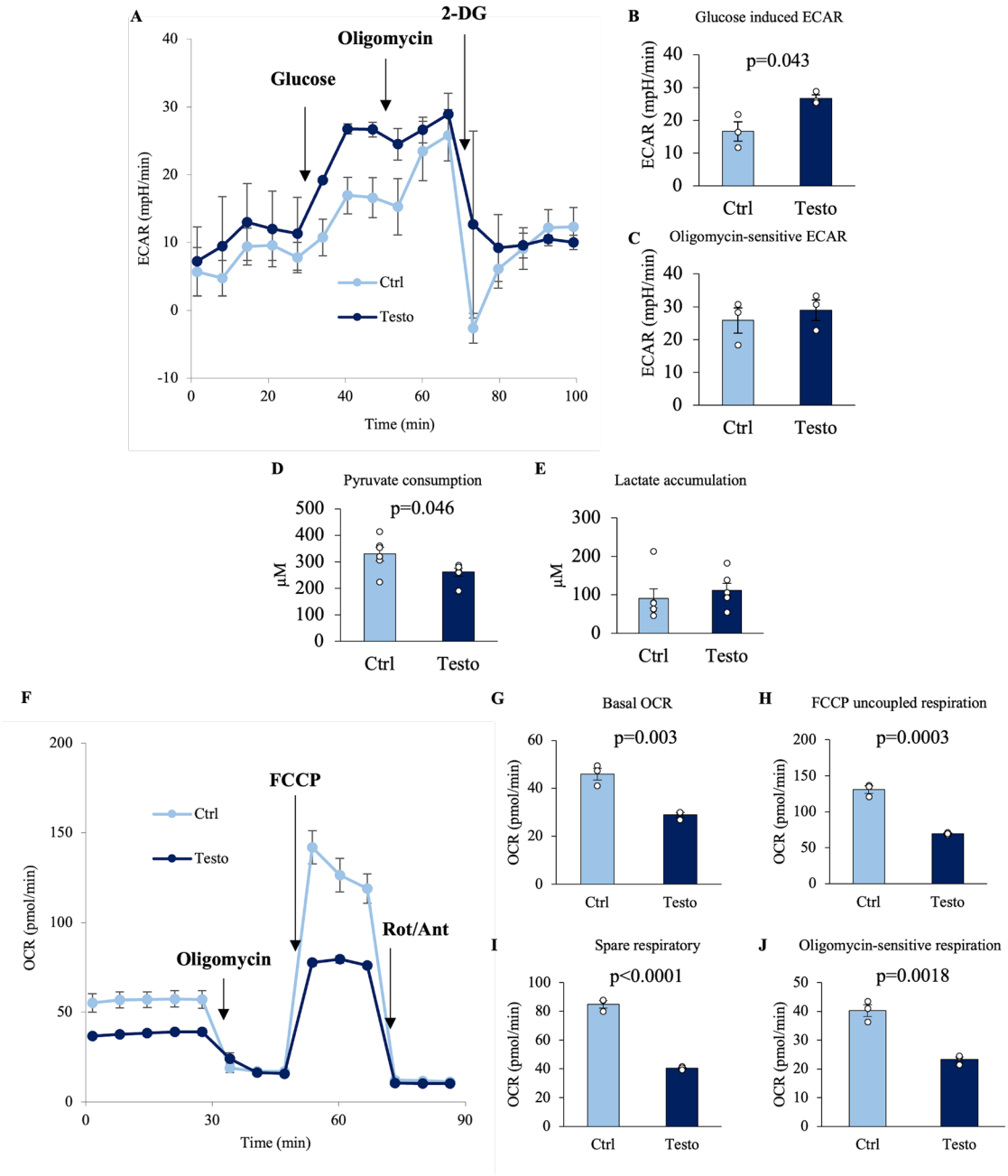

1051

1052 **Figure 4. Testosterone regulates glucose metabolism and mitochondrial ATP production in**
1053 **seminal vesicle epithelial cells.** (A-C) Extracellular acidification rate (ECAR) analysis by an
1054 extracellular flux analyzer in seminal vesicle epithelial cells cultured with 100 ng/mL
1055 testosterone (Testo) or vehicle (Ctrl) for 7 days: (A) ECAR kinetics of seminal vesicle epithelial
1056 cells using an extracellular flux analyzer. (B) Glucose induced ECAR and (C) Oligomycin-
1057 sensitive ECAR. (D,E) The concentrations of pyruvate and lactate in the culture supernatant.

1058 These measurements were normalized based on cell count and viability. (D) Pyruvate
1059 concentration in the medium where seminal vesicle epithelial cells were cultured with or
1060 without testosterone for 24 hours. (E) Lactate concentration. (F-J) Mitochondrial respiration
1061 measurement by an extracellular flux analyzer: (F) Oxygen consumption rate (OCR) kinetics of
1062 seminal vesicle epithelial cells with or without 100 ng/mL testosterone. (G) Basal OCR, (H)
1063 FCCP uncoupled respiration, (I) Spare respiratory capacity and (J) Oligomycin-sensitive
1064 respiration. Data are mean ± SEM of n = 3 replicate experiments with 3-6 wells containing
1065 pooled cells from 3-5 mice or medium. Student's t-test was used to compare Ctrl and Testo. The
1066 cells were normalized to 10,000 viable cells/well immediately before analysis. The viability of
1067 the cells before experiments was 86-93%.
1068

1069 **Fig.5**

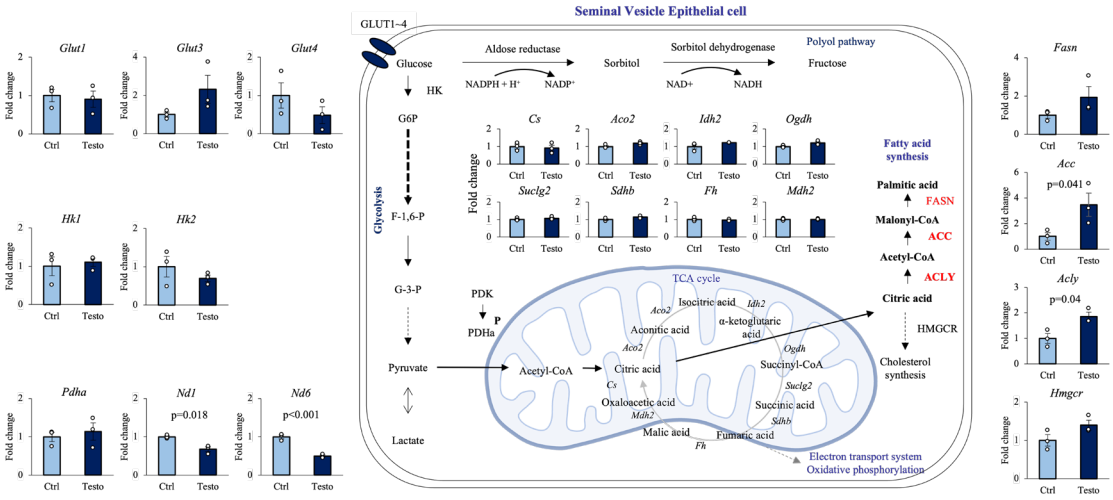

1070

1071 **Figure 5. Effect of testosterone on gene expression of enzymes involved in the glucose**
1072 **metabolic pathway in seminal vesicle epithelial cells.** To elucidate the effects of testosterone
1073 on gene expression of enzymes involved in glucose catabolism and anabolism in seminal vesicle
1074 epithelial cells. ctrl: 7 days of culture with vehicle. Testo: 7 days of culture with 100 ng/mL
1075 testosterone. Data are mean ± SEM of n = 3 replicate experiments with 3-6 wells containing
1076 pooled cells from 3-5 mice. Student's t-test was used to compare Ctrl and Testo.

1077

1078

1079 **Fig.6**

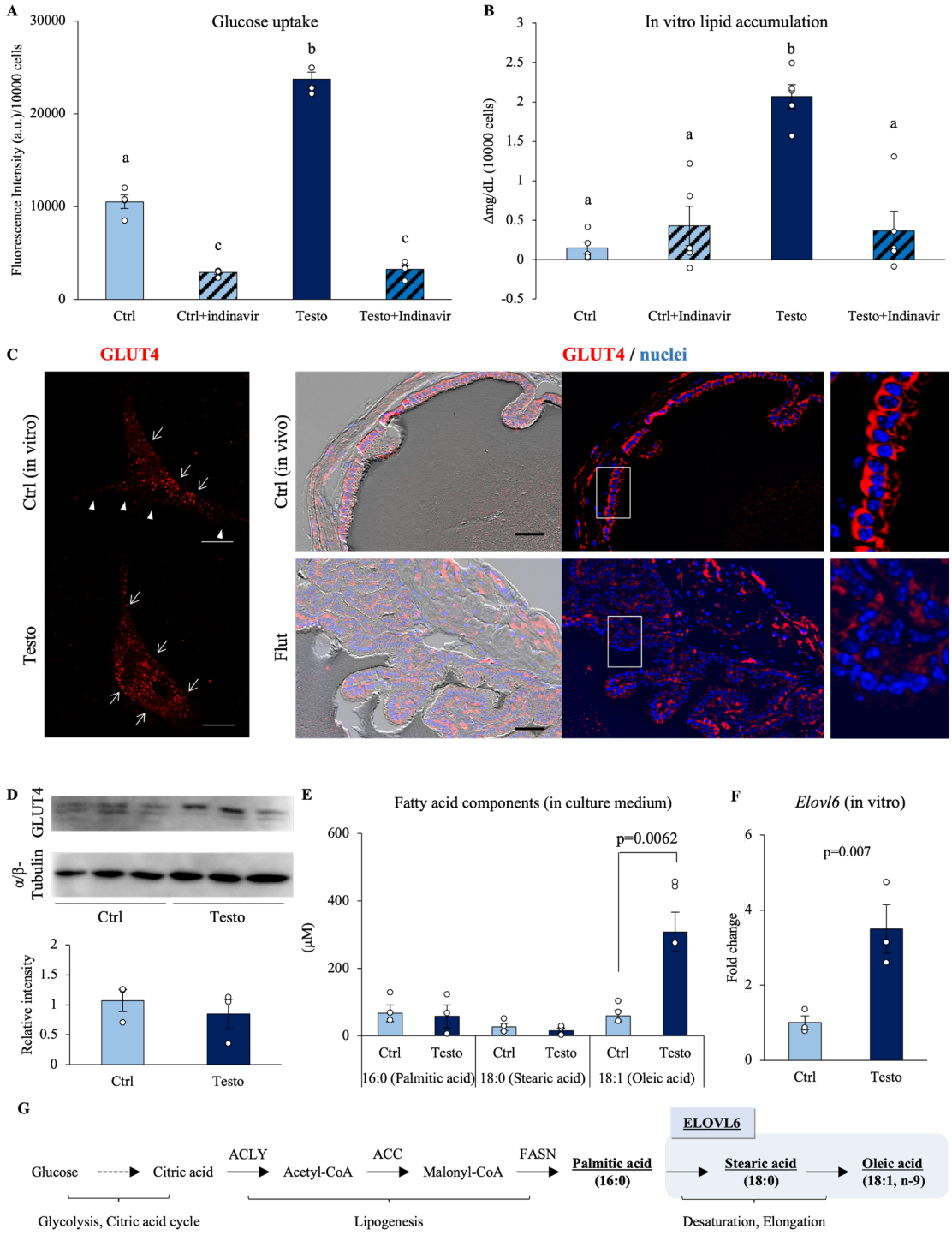

1080

1081 **Fig.6 Testosterone enhances glucose uptake and fatty acid synthesis via GLUT4 trans-**
1082 **localization in seminal vesicle epithelial cells.** (A) The glucose uptake ability of seminal vesicle
1083 epithelial cells was detected using fluorescence-tagged glucose. The cells were cultured with 100

1084 ng/mL testosterone and/or indinavir (100 μM) for 7 days and then further treated with glucose
1085 uptake probe-green for 15 min, and intracellular fluorescence was measured by flow cytometry
1086 (n=4). (B) Lipid accumulation in the medium where seminal vesicle epithelial cells were
1087 incubated for 24 hours (n=6). (C) Immunostaining of GLUT4 in flutamide-treated or vehicle mice
1088 derived seminal vesicle. Scale bar is 50 μm. (D) Western blot images of GLUT4 and α/β-tubulin
1089 in three sets of seminal vesicle epithelial cells cultured with 100 ng/mL testosterone (Testo) or in
1090 vehicle (Ctrl) for 7 days. Quantitative analysis of GLUT4 relative to α-tubulin obtained from
1091 Western blot. (E) Fatty acid composition in the medium was analyzed using gas chromatography.
1092 (F) Quantification of *Elovl* family gene expression by RT-qPCR. (G) Pathway of glucose
1093 assimilation to oleic acid. Data are mean ± SEM. n=3-6 independent replicates. Each replicate
1094 experiments with 3-6 wells containing pooled cells from 3-5 mice or medium. (A,B) The glucose
1095 uptake and lipid measurements were normalized based on cell count and viability. A two-way
1096 ANOVA was performed. Both the Indinavir and testosterone treatment were significant. The
1097 interaction was significant. Tukey's Honest Significant Difference test was performed as a post
1098 hoc test. Different letters represent significantly different groups. Student's t-test was used for
1099 comparison between the two groups.
1100
1101
1102
1103
1104
1105
1106
1107
1108

Fig.7

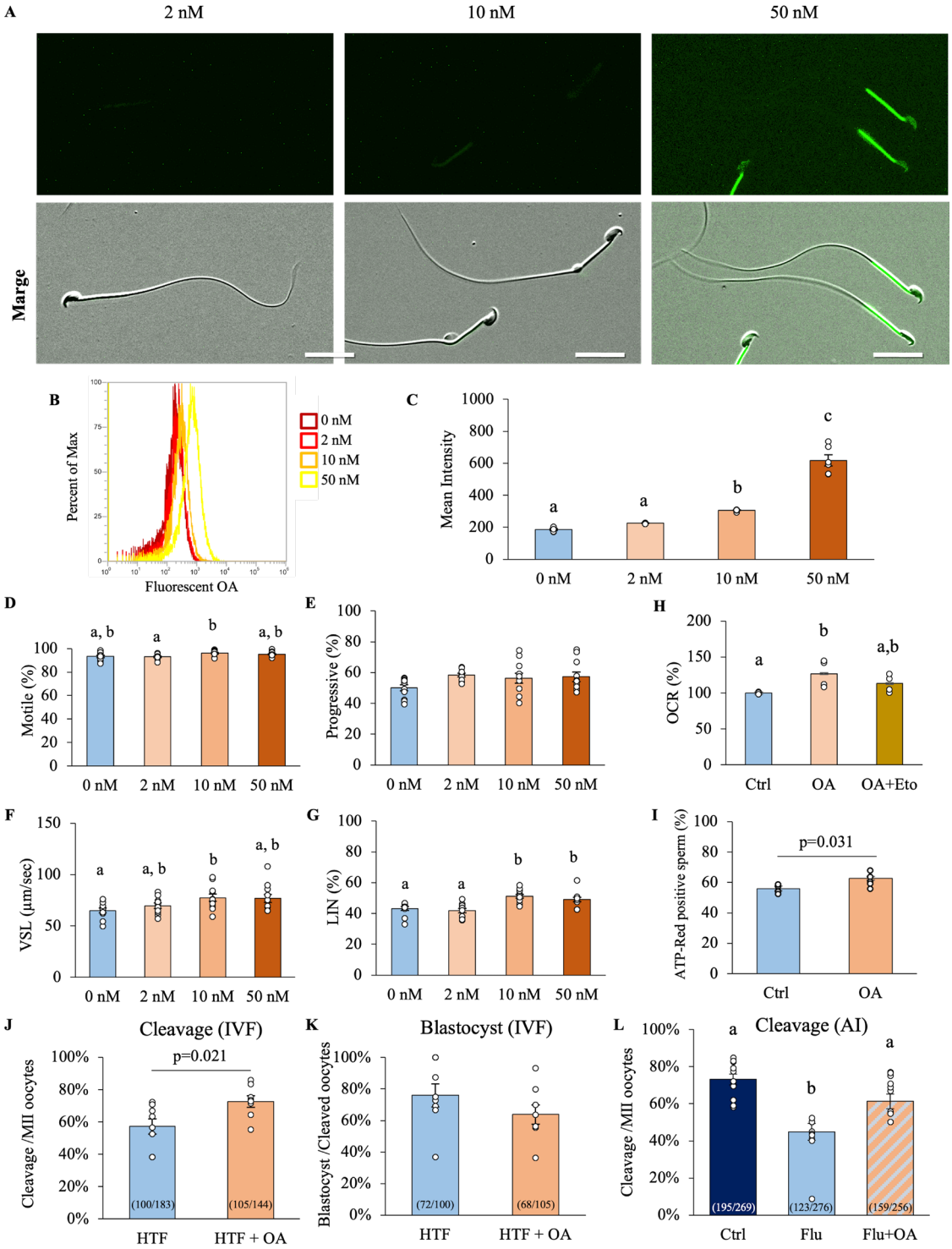
A
2 nM
10 nM
50 nM
Marge
B
Percent of Max
Fluorescent OA
0 nM
2 nM
10 nM
50 nM
C
Mean Intensity
0 nM
2 nM
10 nM
50 nM
D
Motile (%)
E
Progressive (%)
H
OCR (%)
Ctrl
OA
OA+Eto
F
VSL (μm/sec)
G
LIN (%)
I
ATP-Red positive sperm (%)
p=0.031
J
Cleavage (IVF)
Cleavage /MII oocytes
p=0.021
(100/183)
(105/144)
HTF
HTF + OA
K
Blastocyst (IVF)
Blastocyst /Cleaved oocytes
(72/100)
(68/105)
L
Cleavage (AI)
(195/269)
(123/276)
(159/256)
Flu
Flu+OA

1113 **Figure 7. Oleic acid is incorporated to sperm, which enhances linear motility and**
1114 **mitochondrial activity.** (A) Epididymal sperm were incubated with fluorescently labeled oleic
1115 acid (OA) and the fluorescence intensity after quenching was observed by a fluorescence
1116 microscope. (B) The fluorescence intensity of fluorescence-conjugated OA in sperm was
1117 detected by flow cytometry. (C) Average fluorescence intensity of sperm at different
1118 concentrations of fluorescence-conjugated OA. (D-G) OA improved sperm motility parameters.
1119 Sperm collected from mouse epididymis was incubated with OA for 60 min: (D) Motile, (E)
1120 Progressive motile, (F) Straight-Line Velocity; VSL and (G) Linearity; LIN (H) Increase in the
1121 Oxygen consumption rate (OCR) of cultured sperm was measured using flux analyzer after
1122 treatment with 10 nM OA or 10 nM OA + 40 nM Etomoxir (Eto). Ctrl: the sperm cultured in
1123 HTF medium. Each well was seeded with 180 μL of NaHCO3- Free HTF medium containing
1124 3,000,000 sperm. (I) The percentage of ATP-Red positive sperm after 1 hour incubation with or
1125 without 10 nM OA, measured using BioTracker ATP-Red staining and flow cytometry. (J,K)
1126 The sperm, after 1 hour of incubation with or without 10 nM OA, were used for the IVF test and
1127 analyzed for the rate of oocytes reaching cleavage. and blastocyst stage. (J) Cleavage rate. (K)
1128 Blastocyst rate. (L) Artificial insemination using sperm treated for 1 hour with “pseudo”
1129 seminal plasma from control (Ctrl), flutamide-treated (Flu) mice and supplement of 10 nM OA
1130 (Flu+OA) followed by an evaluation of the fertilization rates. Note that the donor mice for
1131 sperm and seminal vesicle secretions were different. Data are mean ± SEM. n=3-11 independent
1132 replicates. Percentage data were subjected to arcsine transformation before statistical analysis.
1133 Differences between groups were assessed by one-way analysis of variance (ANOVA). When
1134 ANOVA was significant, differences among values were analyzed by Tukey's Honest
1135 Significant Difference test for multiple comparisons. Different letters represent significantly
1136 different groups. Student's t-test was used for comparison between the two groups.
1137

1138 **Fig.8**

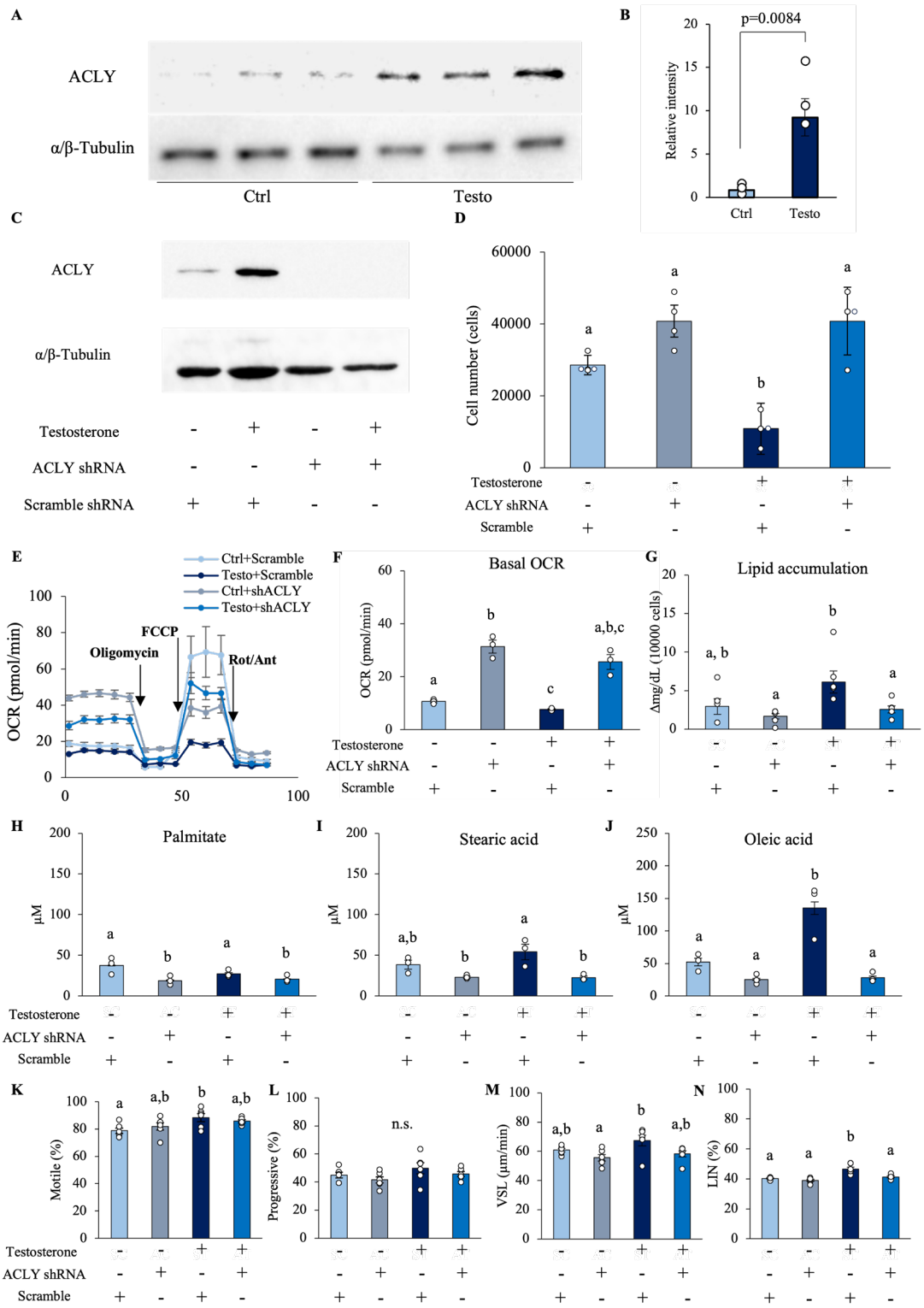

1139

1140 **Figure 8. Testosterone-regulated ACLY induces metabolic shifts in seminal vesicle epithelial**

1141 **cells.** (A) Western blot images of ACLY and α/β-tubulin in three sets of seminal vesicle epithelial

1142 cells cultured with 100 ng/mL testosterone (Testo) or in vehicle (Ctrl) for 7 days. (B) Quantitative
1143 analysis of ACLY relative to α-tubulin obtained from Western blot. (C) siRNA knockdown
1144 experiments of ACLY in seminal vesicle epithelial cells. ACLY protein levels in scrambled
1145 shRNA or ACLY shRNA-transfected seminal vesicle epithelial cells cultured with or without 100
1146 ng/mL testosterone were determined by Western blot. (D) Number of cells at 7 days after
1147 incubation. (E,F) Changes in oxygen consumption of seminal epithelial cells were analyzed by a
1148 flux analyzer: (E) Oxygen consumption rate (OCR) kinetics of seminal vesicle epithelial cells
1149 transfected with scrambled shRNA or ACLY shRNA. (F) Basal OCR. (G) The impact of ACLY
1150 knockdown on testosterone-induced fatty acid synthesis was measured. These measurements
1151 were normalized based on cell count and viability. The viability of the cells before experiments
1152 was 67-81%. (H-I) Fatty acid composition in the cultured supernatants was analyzed using gas
1153 chromatography. (H) Palmitate (C16:0). (I) Stearic acid (C18:0). (J) Oleic acid (C18:1). (K-N)
1154 The effect of culture supernatants of testosterone-treated cells on sperm motility was evaluated,
1155 especially after ACLY knockdown. (K) Motile. (L) Progressive motile. (M) Straight-Line
1156 Velocity; VSL. (N) Linearity; LIN. Data are mean ± SEM. n=3-6 independent replicates.
1157 Repeated experiments were performed with cells recovered from 3 wells containing pooled cells
1158 from 3 to 5 mice. Student's t-test was used for comparison between the two groups. Percentage
1159 data were subjected to arcsine transformation before statistical analysis. (B) Significance was
1160 tested in comparison using Student’s t-test. (D,G-M) A two-way ANOVA was performed. Tukey's
1161 Honest Significant Difference test was performed as a post hoc test. (D) Both the ACLY
1162 knockdown and testosterone treatment were significant. The interaction was significant. (G) Both
1163 the ACLY knockdown and testosterone treatment were significant. The interaction was not
1164 significant. (H,I) Only the ACLY knockdown were significant. The interaction was not significant.
1165 (J) Both the ACLY knockdown and testosterone treatment were significant. The interaction was
1166 significant. (F,N) Since the results of the Bartlett test were significant, a two-way ANOVA using
1167 a generalized linear model was performed. Games-Howell was performed as a post hoc test. (E)
1168 Only the ACLY knockdown were significant. The interaction was not significant. (N)
1169 Testosterone treatment were significant. The interaction was significant. Different letters
1170 represent significantly different groups.
1171

1172 **Fig.9**

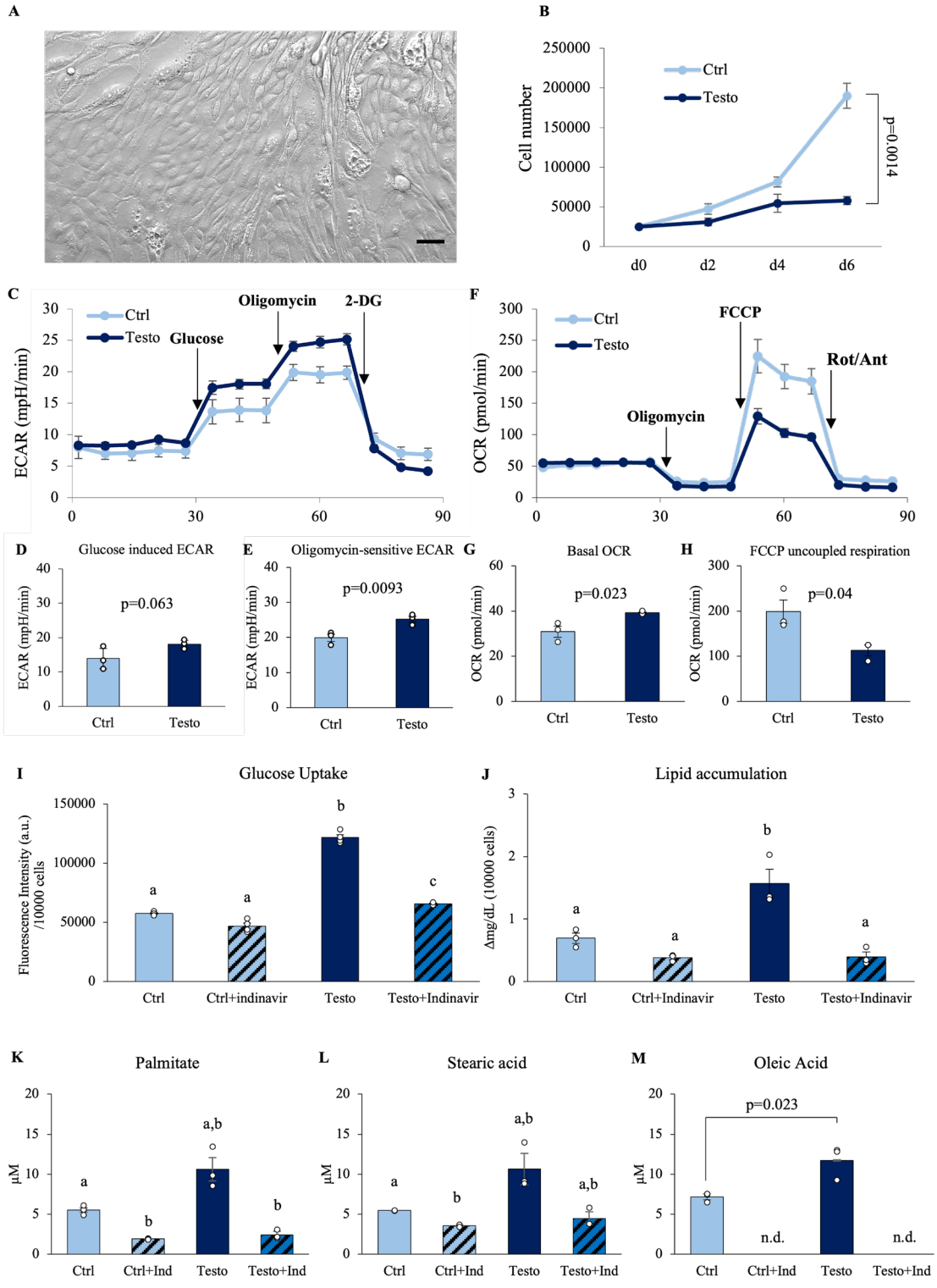

1173

1174 **Figure 9. Testosterone regulates the metabolic activity of human seminal epithelial cells.** (A)

1175 Representative image of human seminal vesicle epithelial cells. (B) Growth curves of seminal

1176 vesicle epithelial cells with 100 ng/mL testosterone (Testo) or without (Ctrl). (C-H) Extracellular
1177 acidification rate (ECAR) kinetics and Oxygen consumption rate (OCR) kinetics of human
1178 seminal vesicle epithelial cells after 6 days of culture with or without 100 ng/mL testosterone
1179 using a flux analyzer. (D) Glucose induced ECAR and (E) Oligomycin-sensitive ECAR. (G) Basal
1180 OCR, (H) FCCP uncoupled respiration. (I) The glucose uptake ability of seminal vesicle epithelial
1181 cells was detected using fluorescence-tagged glucose. (J) Lipid accumulation in the medium
1182 where human seminal vesicle epithelial cells were incubated for 24 hours. (H-I) Fatty acid
1183 composition in the cultured supernatants was analyzed using gas chromatography. (H) Palmitate
1184 (C16:0). (I) Stearic acid (C18:0). (J) Oleic acid (C18:1). Data are mean ± SEM. n=3 independent
1185 replicates. Student's t-test was used for comparison between the two groups. (C-J) These
1186 measurements were normalized based on cell count and viability. The viability of the cells before
1187 experiments was 88-96%. (I,K,L) Since the results of the Bartlett test were significant, a two-way
1188 ANOVA using a generalized linear model was performed. Games-Howell was performed as a
1189 post hoc test. Both the Indinavir and testosterone treatment were significant. The interaction was
1190 significant. (J) A two-way ANOVA was performed. Tukey's Honest Significant Difference test
1191 was performed as a post hoc test. Both the Indinavir and testosterone treatment were significant.
1192 The interaction was significant. Different letters represent significantly different groups.
1193
1194

1195 **Fig.10**

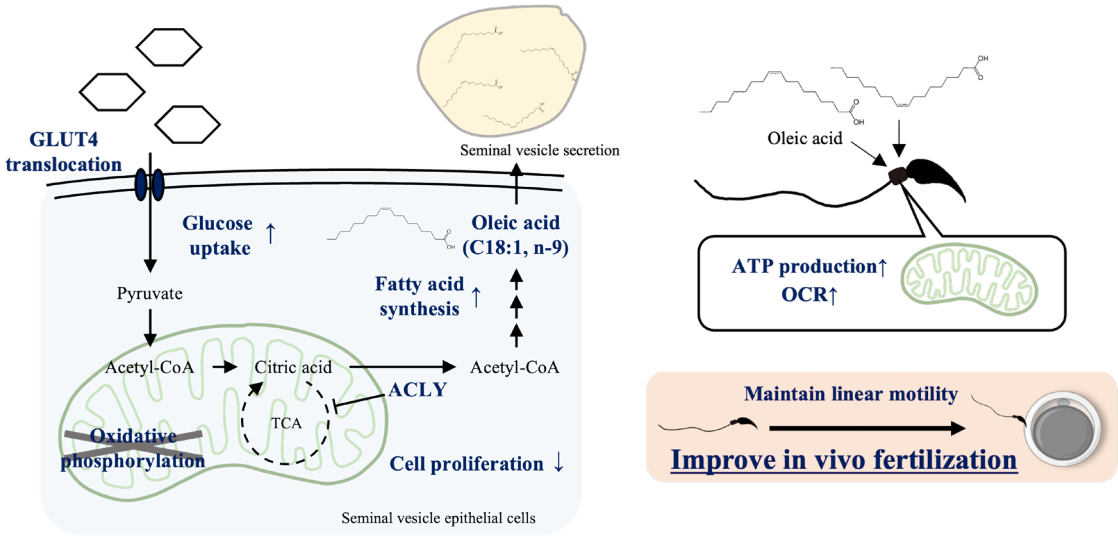

1196

1197 **Figure 10. Metabolic changes in the seminal vesicle epithelial cells by testosterone improve**
1198 **the fertility of sperm.** Left part: Testosterone promotes glucose uptake by changes in the
1199 localization of GLUT4 in seminal vesicle epithelial cells. ATP-citrate-lyase (ACLY) activated by
1200 testosterone promotes fatty acid synthesis by skipping some tricarboxylic acid (TCA) cycle steps.
1201 Simultaneously, cell proliferation in the epididymal epithelial cells is suppressed. Testosterone
1202 also promotes the synthesis of oleic acid from acetyl-CoA synthesized by ACLY. Right part: Oleic
1203 acid, incorporated into the sperm midpiece, increases the oxygen consumption rate (OCR) in
1204 sperm mitochondria and increases ATP production. Therefore, oleic acid in seminal plasma is
1205 important for male fertility because it improves sperm linear motility and fertilization ability.
1206

1207 **Supplemental Figure 1**

A

	Average	SEM
Motility (%)	91.5	7.5
Progressive motile (%)	57.5	6.6
VCL (μm/sec)	190.8	9.4
VSL (μm/sec)	74.7	3.5
LIN (%)	38.0	3.6
Viscosity of HTF (mPa·s)	0.8	0.01

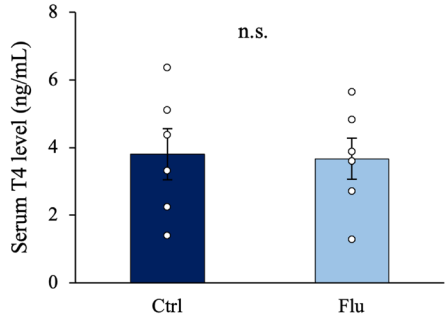

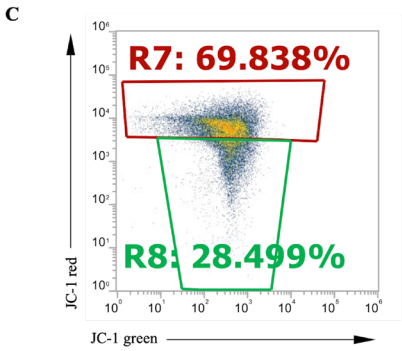

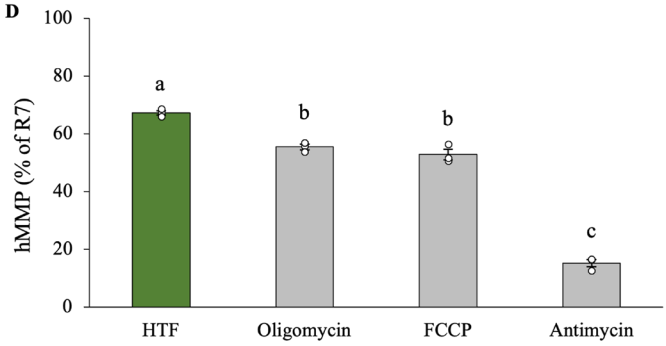

1208

1209 **Supplemental Figure 1. Sperm quality control data and exploratory research into the effects**
1210 **of seminal vesicle secretions on sperm fertilization** (A) The baseline information for the
1211 epididymal sperm used in Fig 1 and Supplemental Fig 2A. Curvi-Linear Velocity; VCL, Straight-
1212 Line Velocity; VSL and Linearity; LIN is the ratio of VSL to VCL of sperm incubated in HTF
1213 medium one hour. (B) Serum testosterone levels in seminal vesicle secretion donors. (C) A
1214 representative flow cytometry pattern of JC-1 staining of sperm that was not treated with drugs
1215 (HTF). (D) The effect of various drugs on the proportion of high mitochondrial membrane
1216 potential (hMMP; R7). Data are mean ± SEM. At least three independent replicates. (B)
1217 Significance was tested in comparison using Student's t-test. (D) Percentage data were subjected
1218 to arcsine transformation before statistical analysis. Differences between groups were assessed
1219 by one-way analysis of variance (ANOVA). When ANOVA was significant, differences among
1220 values were analyzed by Tukey's Honest Significant Difference test for multiple comparisons.
1221 Different letters represent significantly different groups.

1222

1223 **Supplemental Figure 2**

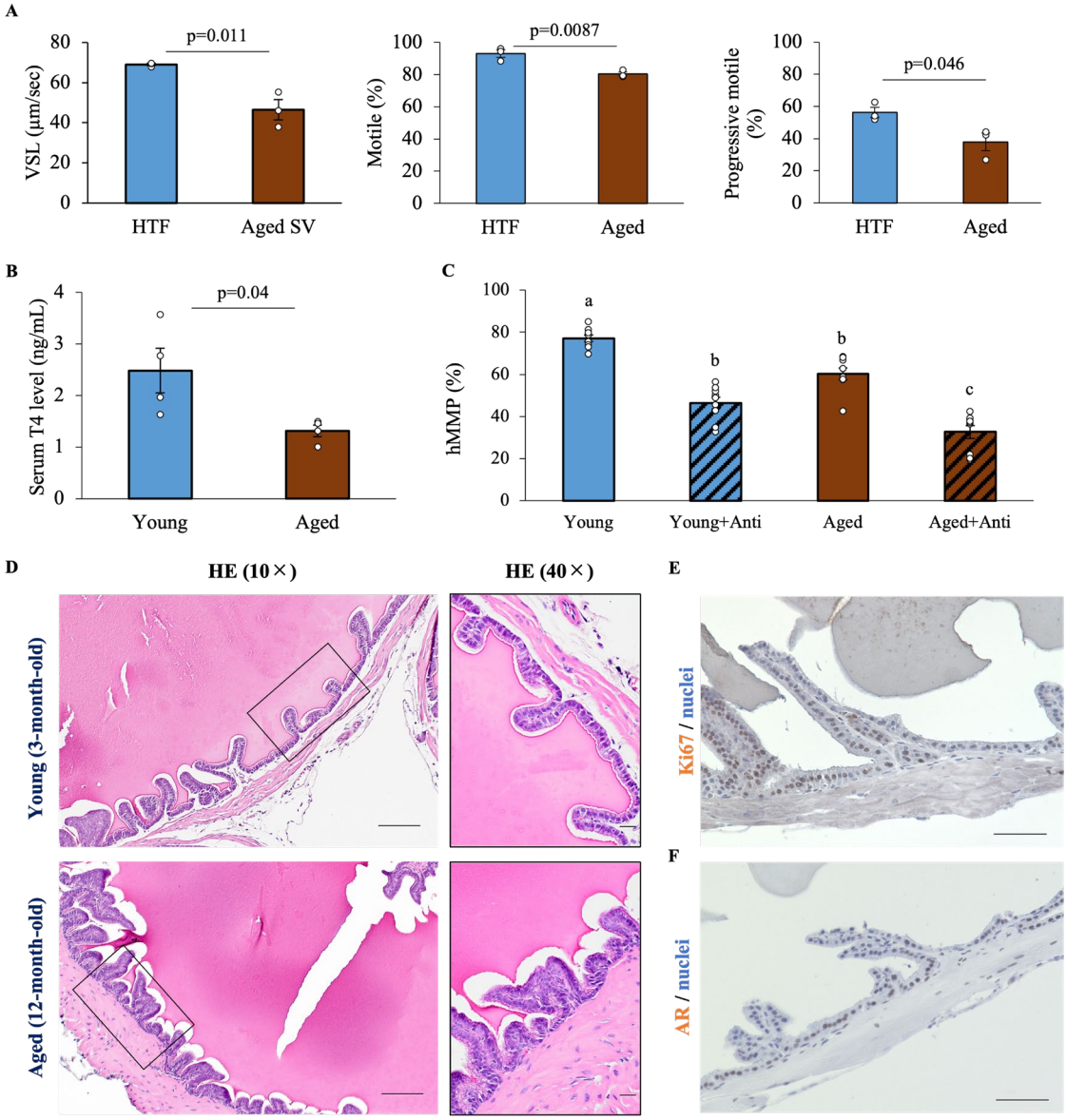

1224

1225 **Supplemental Figure 2. Characteristics of the seminal vesicle in aging mice** (A) The effects
1226 of secretions from aged seminal vesicle fluid on sperm motility. Straight-Line Velocity; VSL,
1227 Motile, and Progressive motile. (B) Serum testosterone (T4) levels in young (3 months old) or
1228 aged (12 months) mice. (C) The high mitochondrial membrane potential (hMMP) was checked
1229 by the JC-1 kit. (D) Hematoxylin/Eosin (HE) staining in seminal vesicles of young and aged
1230 mice. Scale bar=50 μm for left panel and 20 μm for right panel. (E) Representative images
1231 staining for Ki67. Scale bar=50 μm. (F) The localization of the androgen receptor (AR; NR3C4)
1232 in the seminal vesicles of aged mice. Scale bar=50 μm. (E,F) Images were obtained at 10×

magnification. Data are mean ± SEM. At least three independent replicates. Percentage data were subjected to arcsine transformation before statistical analysis. (A,B) Significance was tested in comparison using Student's t-test. (C) A two-way ANOVA was performed. Tukey's Honest Significant Difference test was performed as a post hoc test. Both the age and antimycin treatment were significant. The interaction was not significant. Different letters represent significantly different groups.

1240 **Supplemental Figure 3**

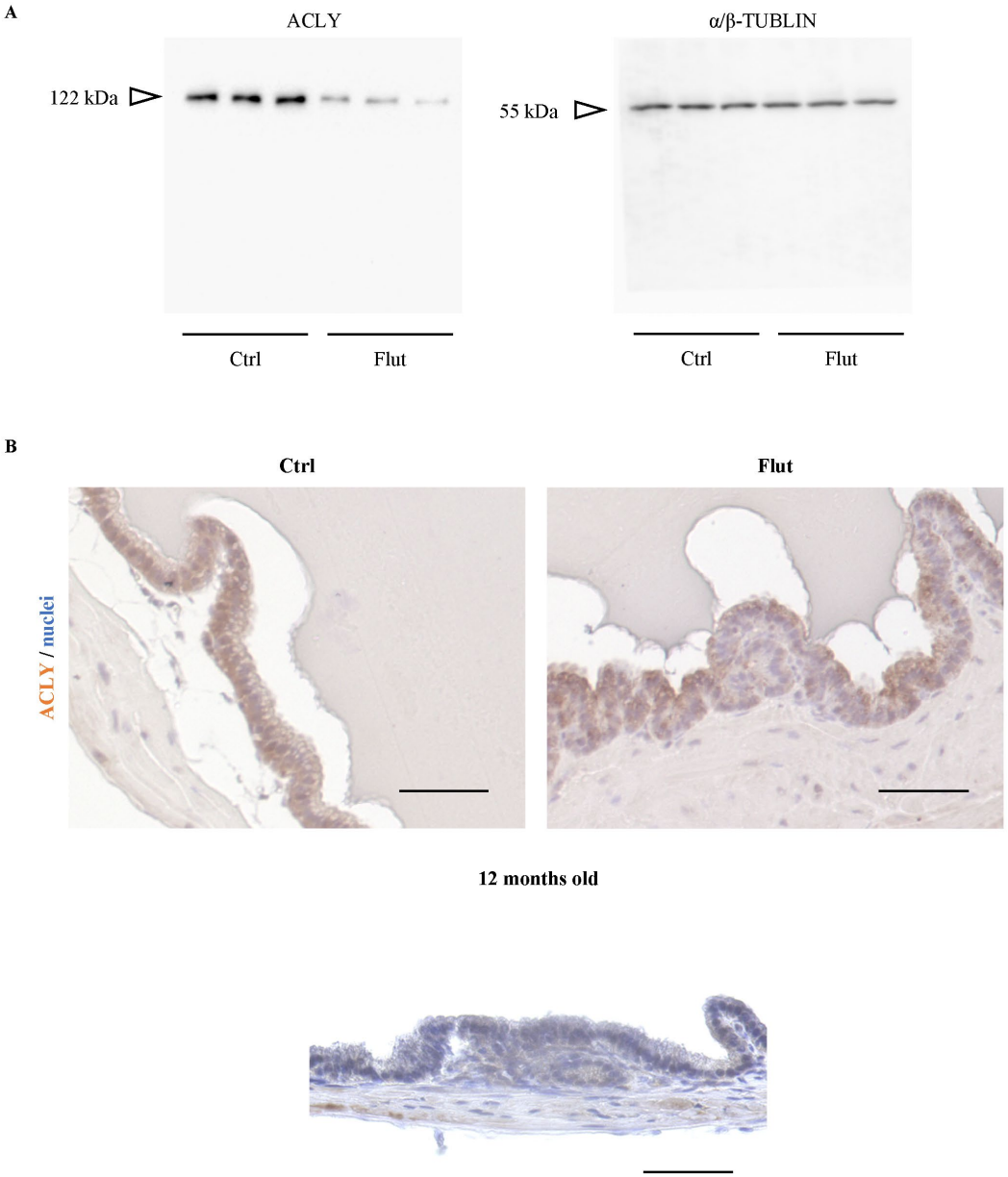

1241

1242 **Supplemental Figure 3. ACLY expression in in vivo seminal vesicle** (A) Representative
1243 Western blot images of ACLY and α-tubulin in three sets of seminal vesicle collected from 50
1244 mg/kg flutamide subcutaneously for 7 days (Flut) or vehicle treated mice (Ctrl). (B) ACLY
1245 immunostaining: seminal vesicles from wild-type mice, flutamide-treated mice, and 12-month-
1246 old aging mice. Scale bar is 50 µm.

1247

1248

1249 **Supplemental Figure 4**

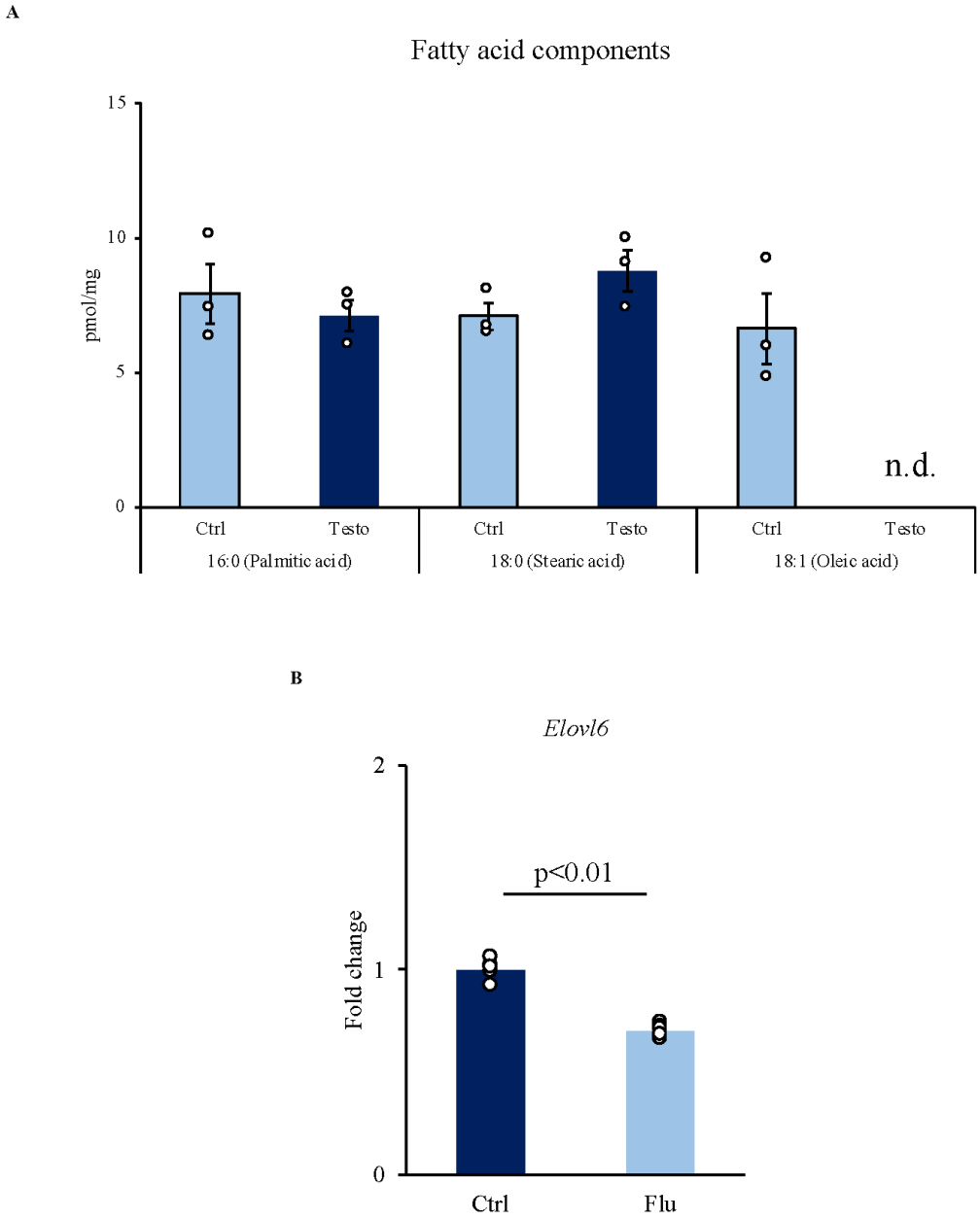

1250

1251 **Supplemental Figure 4. Oleic acid synthesis in vivo regulated by the testosterone-androgen**
1252 **receptor system** (A) Fatty acid composition of seminal vesicle extracts in flutamide-treated (Flu)
1253 or vehicle mice (Ctrl) pretreated with a methylation kit was analyzed by gas chromatography.
1254 *Moles contained per unit wight of seminal vesicle secretions. (B) Quantification of *Elovl6* gene
1255 expression by RT-qPCR. Data are mean ± SEM. Student's t-test was used for comparison between
1256 the two groups (n=5).

1257

1258 **Supplemental Figure 5**

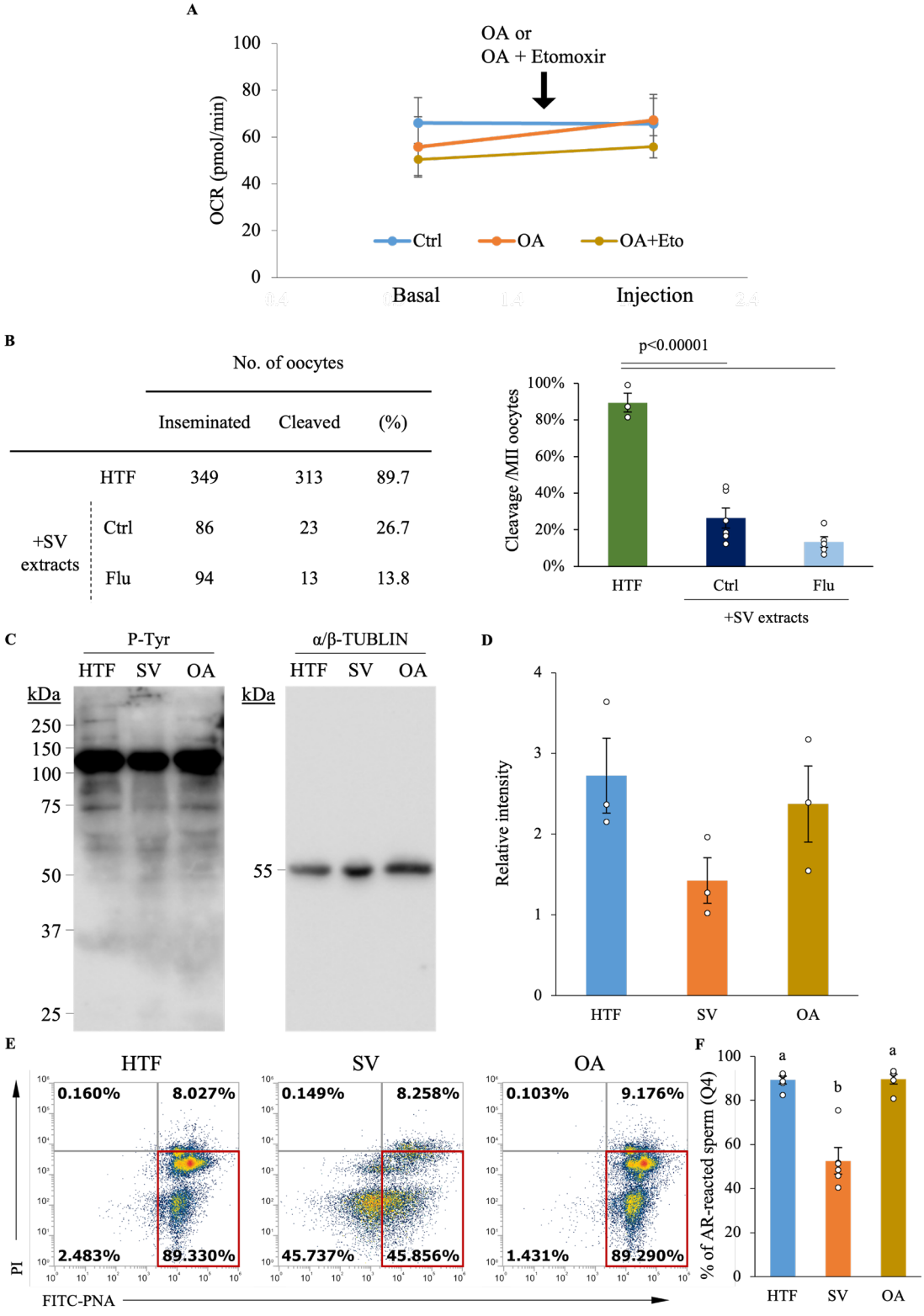

1259

1260 **Supplemental Figure 5. The effects of oleic acid and seminal vesicle secretions on sperm**
1261 **function** (A) Tracing of oxygen consumption rate (OCR) basal and injection with 10 nM oleic
1262 acid (OA) or OA + 40 nM Etomoxir (Eto). (B) The sperm, after 1 hour of incubation with or
1263 without seminal vesicle secretions (SV) from nontreated (Ctrl) or flutamide-treated mice(Flu),
1264 were used for IVF, and the cleavaged oocytes were observed. The absolute number of oocytes
1265 collected from the oviduct and the cleavage rate are shown. (C) Western blot analysis for
1266 phosphotyrosine (P-Tyr) in capacitated spermatozoa (Ctrl; 1-hour incubation in HTF medium)
1267 and treated with SV from healthy mice or 10 nM oleic acid (OA). (D) Quantitative analysis of
1268 GLUT4 relative to α-tubulin obtained from Western blot. (E) Flow cytometric analysis of the
1269 sperm after 1 hour incubation in control medium (HTF) and medium containing SV or 10 nM OA,
1270 using fluorescein isothiocyanate-conjugated peanut agglutinin (PNA-FITC; to distinguish
1271 between acrosome-reacted and non-reacted cells) and propidium iodide (PI; to distinguish
1272 between dead and viable cells). (F) The percentage of viable sperm with an acrosome reaction
1273 (PI-, PNA-FITC+) was evaluated by flow cytometry in the 4th quadrant (4Q; red square). Data
1274 are mean ± SEM. At least three independent replicates. Percentage data were subjected to arcsine
1275 transformation before statistical analysis. (B) Dunnett's test was used to analyze the cleavage rate.
1276 Different letters represent significantly different groups. (D,F) Differences between groups were
1277 assessed by one-way analysis of variance (ANOVA). When ANOVA was significant, differences
1278 among values were analyzed by Tukey's Honest Significant Difference test for multiple
1279 comparisons.
1280
1281

1282 **Supplemental Figure 6**

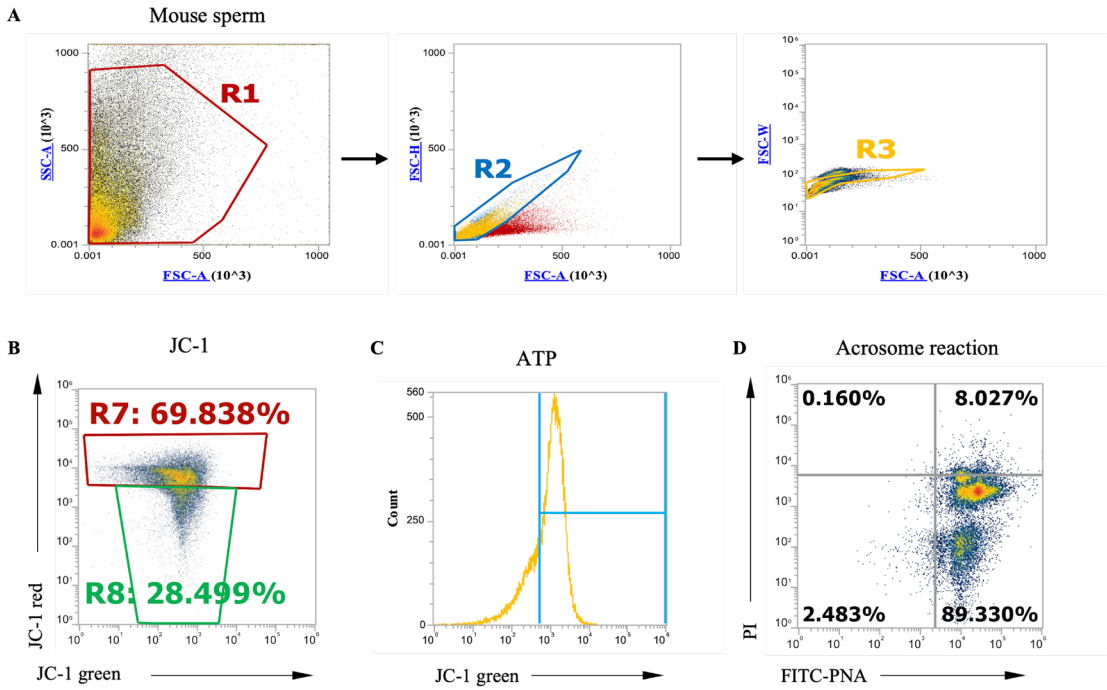

1283

1284 **Supplemental Figure 6. Gating strategy of flow cytometry for sperm** (A) Gating strategy for
1285 the selection of single sperm. Using forward scatter (FSC)-A and side scatter (SSC)-A dot plots,
1286 similar size and complexity cells were firstly selected (R1). In FSC-A and FSC-H dot plots and
1287 FSC-A and FSC-W dot plots, similar-size cells were accumulated near area; thus, using these
1288 plots, again similar-size cells were selected (R2, R3). The cells in R3 were used for below
1289 analysis. (B) The dot plots of 5,5’,6,6’-tetrachloro-1,1’,3,3’-tetraethylbenzimidazolyl
1290 carbocyanine iodide (JC-1) green (x-axis) and red (y-axis). The percentage of JC-1 red-
1291 positive sperm (R7) was used for the analysis. (C) Histograms of BioTracker Red staining.
1292 Blue line indicates the range of positive cells used in Figure 7I. (D) The dot plots of
1293 fluorescein isothiocyanate-conjugated peanut agglutinin (PNA-FITC; x-axis) and
1294 propidium iodide (PI; y-axis).

1295

1296 **Supplemental Figure 7**

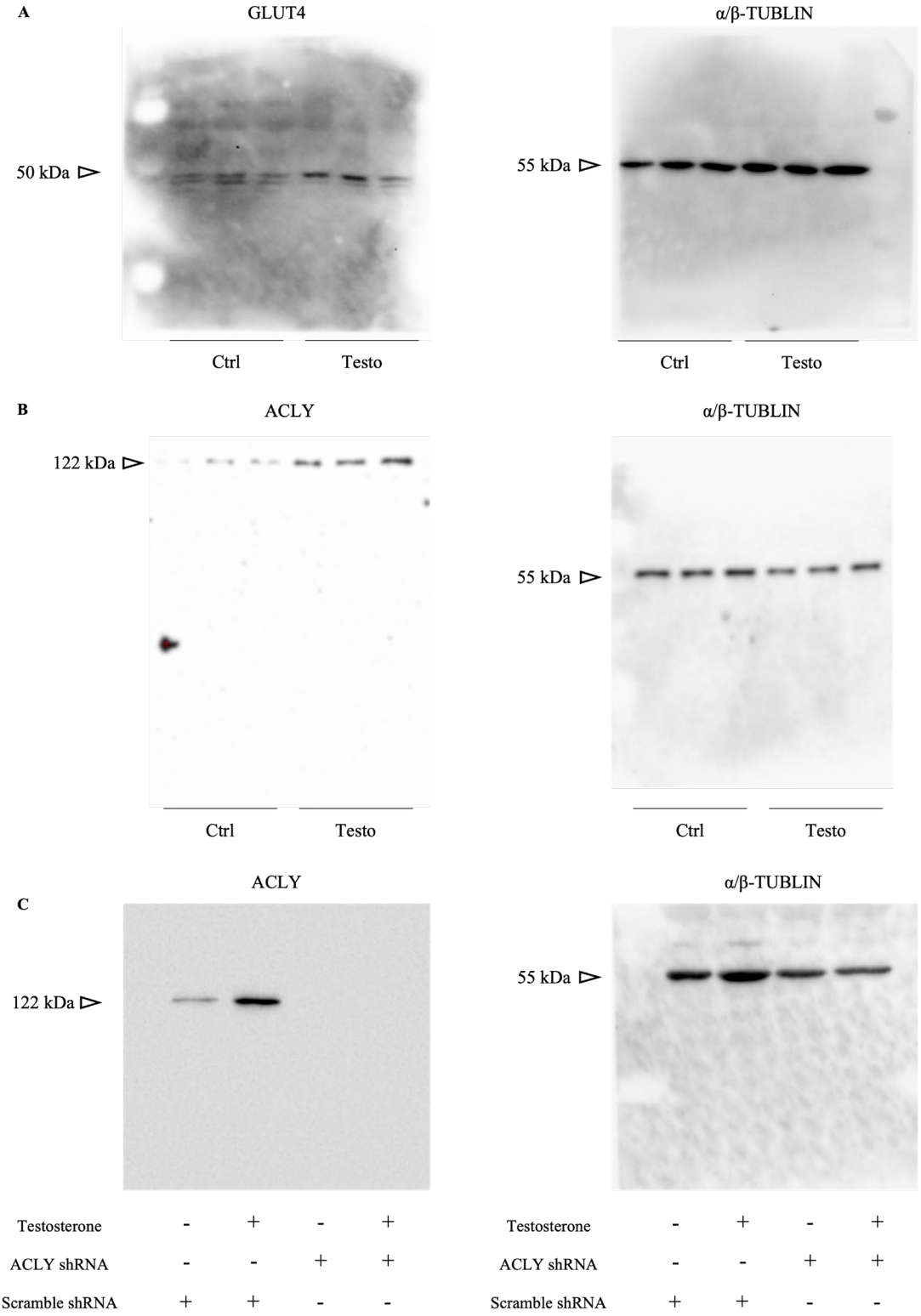

1297

1298 **Supplemental Figure 7. Full-length blotting images of western blotting** (A) Full-length

1299 blotting images of GLUT4 and α/β-TUBLIN in seminal vesicle epithelial cells cultured with

1300 100 ng/mL testosterone (Testo) or in vehicle (Ctrl) in Figure 6D. (A) Full-length blotting images
1301 of ACLY and α/β-TUBLIN in seminal vesicle epithelial cells cultured with 100 ng/mL
1302 testosterone (Testo) or in vehicle (Ctrl) in Figure 8A. (B) Full-length blotting images of ACLY
1303 and α/β-TUBLIN in seminal vesicle epithelial cells in Figure 8C. ACLY protein levels in
1304 scrambled shRNA or ACLY shRNA-transfected seminal vesicle epithelial cells cultured with or
1305 without 100 ng/mL testosterone were determined by Western blot.
1306

1307 **Supplemental Figure 8**

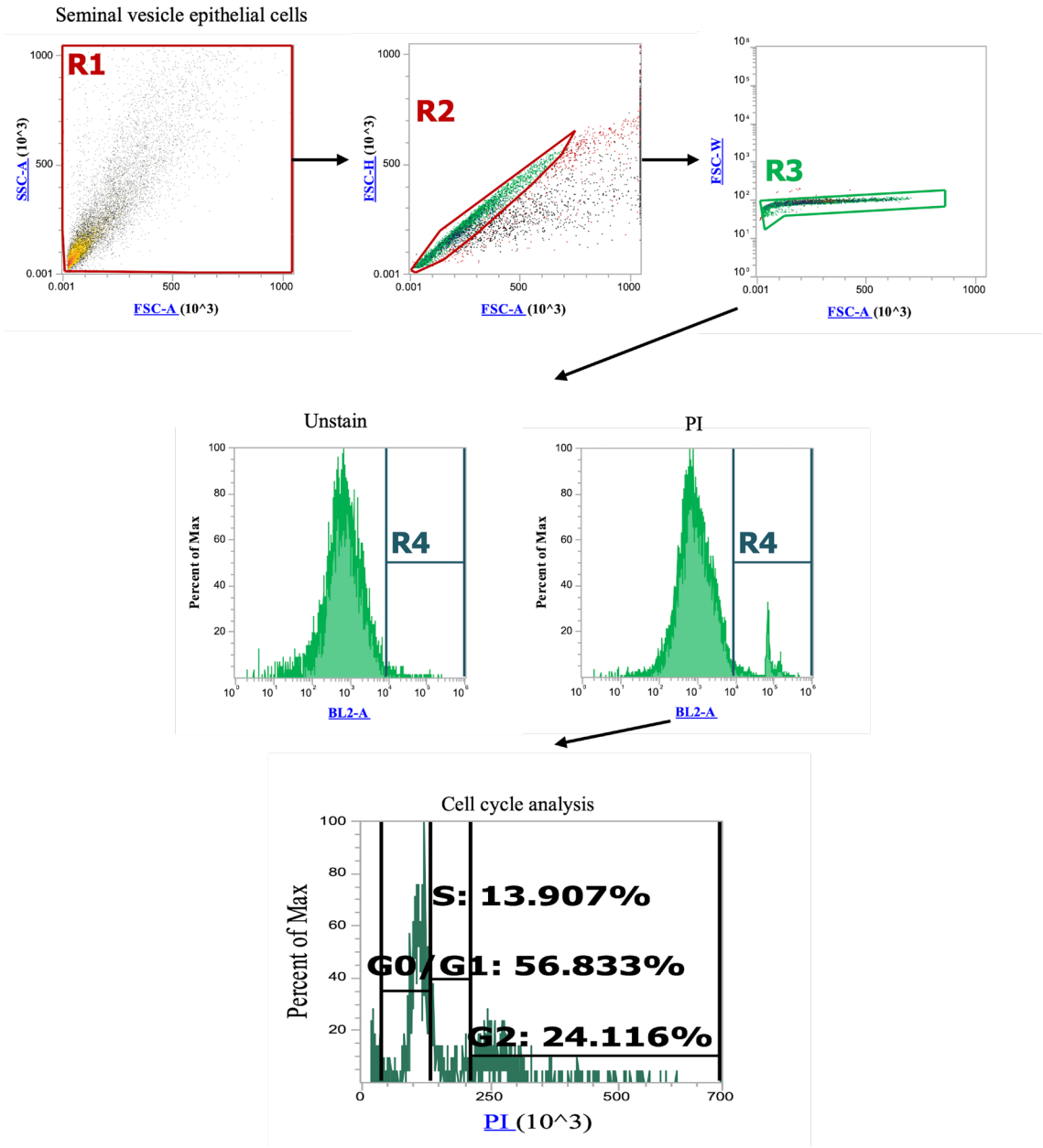

1308

1309 **Supplemental Figure 8. Gating strategy of flow cytometry for seminal vesicle epithelial cells**
1310 Gating strategy for the selection of single sperm. Using forward scatter (FSC)-A and side scatter
1311 (SSC)-A dot plots, similar size and complexity cells were firstly selected (R1). In FSC-A and
1312 FSC-H dot plots and FSC-A and FSC-W dot plots, similar-size cells were accumulated near area;
1313 thus, using these plots, again similar-size cells were selected (R2, R3). The cells in R3 were
1314 applied to the propidium iodide (PI) histogram plot. Labelling DNA with PI allows fluorescence-
1315 based analysis of the cell cycle. The intensity of PI fluorescence correlates with the amount of

1316 DNA in each cell. Comparing the G1 and G2 phases, the amount of DNA doubles in the G2 phase,
1317 so the fluorescence intensity of the cell population also doubles.
1318

Table S1. Primer sequences used for quantitative real-time PCR.

Gene	Forward primer (5'→3')	Reverse primer (5'→3')
Acc	GCCTCTTCCTGACAAACGAG	TGACTGCCGAAACATCTCTG
Acly	AGGTCTCTCTGCAGCCATGT	AAGCTTTCCTCGACGTTTGA
Aco2	CTAGCCTCAGCCCAGTGAAC	CCTTCAGCCACCAGTGAAAT
Cs	CAGATGCCCACAGAGGAACA	AGCTTGGCAATGAGGTCCAT
ElovI6	CCCGAACTAGGTGACACGAT	CCGCAAGGCGTAGTAAGAGT
Fasn	AGCACACATCCTAGGCATCC	TGTCGTGTCAGTAGCCGAGT
Fh	AGCAATGCATATTGCTGCTG	CGCATACTGGACTTGCTGAA
Glut1	AAACATGGAACCACCGCTAC	AGGCCAACAGGTTCATCATC
Glut2	GCCTGTGTATGCAACCATTG	TGGCCCAATCTCAAAGAAAC
Glut3	TGTCACAGGAGAAGCAGGTG	GCTCCAATCGTGGCATAGAT
Glut4	ACTCTTGCCACACAGGCTCT	AATGGAGACTGATGCGCTCT
Hk1	TATCGGTCCAGCACGTATGC	ACATCGTGACCCACACAGTC
Hk2	GGGTAGCCACGGAGTACAAA	TGGATTGAAAGCCAACTTCC
Hmgcr	TGGAGATCATGTGCTGCTTC	GCGACTATGAGCGTGAACAA
Idh2	CCGTCTTCAGAGAGCCAATC	GAAATGGACTCGTCGGTGTT
Mdh2	GCTTTGTCTTCTCCCTCGTG	CAAAGTCCTCGCCTTTCTTG
Nd1	CAGGATGAGCCTCAAACTCC	CCGGTTTGTTTCTGCTAGGG
Nd6	GGTTGGTTGTCTTGGGTTAGC	TAGATCCCCAAGTCTCTGGA
Ogdh	ACATGGCACAGTGCATCATT	ACATCTGCAGAAACCGCTCT
Pdha	GGGGACGTCTGTTGAGAGAG	TGTGTCCATGGTAGCGGTAA
Sdhb	ACTGGTGGAACGGAGACAAG	GTTAAGCCAATGCTCGCTTC
Suclg2	CTTTGGTGGGATCGTCAACT	AACAGCTTTCTTGGCTGCAT
L19	GGCATAGGGAAGAGGAAGG	GGATGTGCTCCATGAGGATGC

1319